

STMAC: Spatio-Temporal Coordination-Based MAC Protocol for Driving Safety in Urban Vehicular Networks

Jaehoon Jeong, *Member, IEEE*, Yiwen Shen, *Student Member, IEEE*, Sangsoo Jeong, *Student Member, IEEE*, Sejun Lee, *Student Member, IEEE*, Hwanseok Jeong, *Student Member, IEEE*, Tae Oh, *Senior Member, IEEE*, Taejoon Park, *Member, IEEE*, Muhammad Usman Ilyas, *Member, IEEE*, Sang Hyuk Son, *Fellow, IEEE*, and David H. C. Du, *Fellow, IEEE*

Abstract—In this paper, we propose a spatio-temporal coordination-based media access control (STMAC) protocol for efficiently sharing driving safety information in urban vehicular networks. STMAC exploits a unique spatio-temporal feature characterized from a geometric relation among vehicles to form a line-of-collision graph, which shows the relationship among vehicles that may collide with each other. Based on this graph, we propose a contention-free channel access scheme to exchange safety messages simultaneously by employing directional antenna and transmission power control. Based on an urban road layout, we propose an optimized contention period schedule by considering the arrival rate of vehicles at an intersection in the communication range of a road-side unit to reduce vehicle registration time. Using theoretical analysis and extensive simulations, STMAC outperformed legacy MAC protocols especially in a traffic congestion scenario. In the congestion case, STMAC can reduce the average superframe duration by 66.7%, packet end-to-

end delay by 68.3%, and packet loss ratio by 88% in comparison with the existing MAC protocol based on the IEEE 802.11p.

Index Terms—Vehicular networks, spatio-temporal, safety, MAC protocol, coordination.

I. INTRODUCTION

DRIVING safety is one of the most important issues since approximately 1.24 million people die each year globally as a result of traffic accidents. Vehicular ad hoc networks (VANETs) have been highlighted and implemented during the last decade to support wireless communications for driving safety in road networks [1], [2]. Driving safety can be improved by an assistance of rapid exchanged of driving information among neighboring vehicles. As an important trend, dedicated short-range communications (DSRC) [3] were standardized as IEEE 802.11p in 2010 (now incorporated into IEEE 802.11 protocols [4]) for wireless access in vehicular environments (WAVE) [2], [5]. IEEE WAVE protocol is a multichannel MAC protocol [4], adopting the enhanced distributed channel access (EDCA) [5] for quality of service (QoS) in vehicular environments. Many research results [6]–[9] published that a performance of WAVE deteriorates when a density of vehicles is high, approaching the performance of a slotted ALOHA process [8]. As a result, many other MAC protocols [10]–[16] have been proposed to improve the performance of WAVE. However, the MAC protocols were not designed to support the geometric relation among vehicles for the driving safety and didn't consider the configuration of urban roads.

A MAC protocol can operate in a distributed coordination function (DCF) mode (i.e., contention based), a point coordination function (PCF) mode (i.e., contention-free based) or a hybrid coordination function (HCF) mode [4]. For driving safety in vehicular environments, a MAC protocol in the DCF-mode executes based on carrier sense multiple access with collision avoidance (CSMA/CA) [4] mechanism. This distributed approach can incur high frame collision rates at congested intersections in an urban area [6]–[9], and in the case of a lack of comprehensive vehicle traffic. As a result, it may lead to an unreliable, non-prompt data exchange. On the contrary, a MAC protocol in the PCF-mode can wield roadside units (RSUs) or access points (APs) as coordinators to

Manuscript received September 19, 2016; revised March 4, 2017 and May 24, 2017; accepted July 2, 2017. This work was supported in part by the Basic Science Research Program through the National Research Foundation of Korea (NRF) funded by the Ministry of Science, ICT & Future Planning (MSIP) under Grant 2014R1A1A1006438, in part by the Ministry of Education under Grant 2017R1D1A1B03035885, and in part by the Global Research Laboratory Program through the NRF and the DGIST Research and Development Program (CPS Global Center) funded by the MSIP under Grant 2013K1A1A2A02078326. The Associate Editor for this paper was L. Li. (*Corresponding author: Sang Hyuk Son.*)

J. Jeong is with the Department of Interaction Science, Sungkyunkwan University, Suwon 16419, South Korea (e-mail: pauljeong@skku.edu).

Y. Shen and H. Jeong are with the Department of Computer Science & Engineering, Sungkyunkwan University, Suwon 16419, South Korea (e-mail: chrishshen@skku.edu; harryjeong@skku.edu).

S. Lee is with the Korea Electronics Technology Institute, Seongnam-si 13509, South Korea (e-mail: sejunlee@skku.edu).

S. Jeong and S. H. Son are with the Department of Information and Communication Engineering, DGIST, Daegu 42988, South Korea (e-mail: 88jeongss@dgist.ac.kr; son@dgist.ac.kr).

T. Oh is with the Department of Information Sciences & Technologies, Rochester Institute of Technology, Rochester, NY 14623-5603 USA (e-mail: tom.oh@rit.edu).

T. Park is with the Department of Robotics Engineering, Hanyang University, Seoul 04763, South Korea (e-mail: taejoon@hanyang.ac.kr).

M. U. Ilyas is with the Department of Electrical Engineering, National University of Sciences and Technology, Islamabad 44000, Pakistan, and also with the Department of Computer Science, Faculty of Computing and Information Technology, University of Jeddah, Jeddah 21589, Saudi Arabia (e-mail: usman.ilyas@seecs.edu.pk; milyas@uj.edu.sa).

D. H. C. Du is with the Department of Computer Science & Engineering, University of Minnesota, Minneapolis, MN 55455 USA (e-mail: du@cs.umn.edu).

Color versions of one or more of the figures in this paper are available online at <http://ieeexplore.ieee.org>.

Digital Object Identifier 10.1109/TITS.2017.2723946

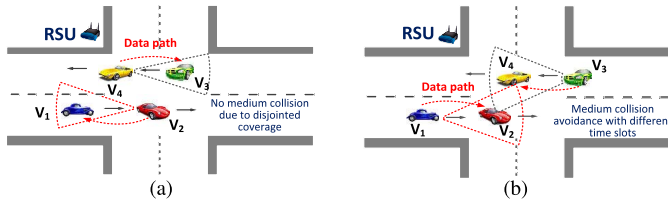


Fig. 1. Spatial and temporal coordination. (a) Spatial coordination. (b) Temporal coordination.

a temporal feature by which the communications should be separated for collision avoidance. Further, based on the urban road layout, we propose a scheme that optimizes the contention period for vehicle registration into an RSU by reducing the contention duration by considering the vehicle arrival rate at an intersection. Our STMAC can facilitate the rapid exchange of driving information among neighboring vehicles. This rapid exchange can help drivers to get driving assistance information for avoiding possible collisions. Even in self-driving, STMAC can help autonomous vehicles avoid collision by exchanging the mobility information and cooperating with each other for driving coordination.

The contributions of this paper are as follows:

- **An LoC graph based channel access scheme via an enhanced set-cover algorithm is proposed:** STMAC's set-cover algorithm handles an *unfixed* subsets family of elements where each subset is covered by a time slot, and each element is a transmission, which differs from the legacy set-cover algorithm [21] handling a *fixed* subset family of elements. This algorithm schedules multiple vehicles to transmit their safety messages simultaneously in spatially disjointed transmission areas (see Section IV-A).
- **A contention period optimization is proposed for the efficient channel usage:** STMAC's contention period adapts the vehicle arrival rate at an intersection in an urban area for better channel utilization. This optimization is feasible in vehicular networks where vehicles move along confined roadways (see Section IV-B).
- **A new hybrid MAC protocol is proposed using spatio-temporal coordination:** STMAC uses the PCF mode to register vehicles for a time slot allocation as well as an emergency message dissemination from an RSU to vehicles. It uses the DCF mode for both safety message exchange and emergency message dissemination among vehicles by *spatio-temporal coordination*. (see Section V).

Through theoretical analysis and extensive simulations, it is shown that STMAC outperforms other state-of-the-art protocols in terms of average superframe duration, end-to-end (E2E) delay, and packet loss ratio.

The remainder of this paper is organized as follows. In Section II, related work is summarized along with analysis. Section III discusses the assumptions and scenarios used for problem formulation. Section IV describes the characterization of spatial-temporal features and the optimization of the contention period. In Section V, the STMAC protocol is proposed. In Section VI, we evaluate STMAC by comparing with baseline MAC protocols (*i.e.*, PCF and DCF MAC protocols) through theoretical data and simulation results. Finally, Section VII concludes this paper along with future work.

II. RELATED WORK

IEEE 802.11 [4] defines an HCF-mode to use a contention-based channel access method for contention-based transfer, called the enhanced distributed channel access (EDCA), and a controlled channel access for contention-free transfer, called

59 schedule time slots for transmitters. This centralized approach
60 can reduce frame collision rates and guarantees a certain
61 delay bound, but increases a data delivery delay since multiple
62 transmitters must be managed. The HCF mode, which is a part
63 of IEEE 802.11 [4], combines the PCF and DCF modes with
64 QoS enhancement feature to deliver QoS data from vehicles
65 to an RSU (*i.e.*, AP). The HCF mode employs the HCF
66 controlled channel access (HCCA) [4] as the PCF-mode for
67 contention-free transfer, and the EDCA [4] mechanism as the
68 DCF-mode for contention-based transfer. However, tailoring
69 optimal combination of the PCF and DCF modes still remains
70 challenging research issues for the driving safety in vehicular
71 environment.

72 On the other hand, for efficient communication among
73 vehicles, RSUs are expected to be deployed at intersections
74 and streets in vehicular networks [17]. RSUs with powerful
75 computation capabilities can operate as edge devices [18] to
76 coordinate channel access for vehicles while preventing channel
77 collision and provides Internet connectivity to disseminate
78 safety information. Thus, a cost for RSU implementation can
79 be easily justified by the reduction of human injuries and
80 deaths as well as property loss caused by road accidents. Also,
81 the implementation of geographical positioning system (GPS)
82 is another important trend in vehicular networks. Navigators
83 (*i.e.*, a dedicated GPS navigator [19] and a smartphone
84 navigation app [20]) are commonly used by drivers who are
85 driving to destinations in unfamiliar areas. An RSU can collect
86 GPS data of vehicles in its coverage so that the transmission
87 schedule of vehicles can be optimized. Therefore, RSUs can
88 be used as coordinators to orchestrate communications among
89 vehicles. However, few studies have explored the important
90 functions of RSUs for driving safety.

91 In this paper, we propose a Spatio-Temporal coordination
92 based MAC (STMAC) protocol for urban scenarios, utilizing
93 a spatio-temporal feature and a road layout feature in
94 urban areas for better wireless channel access in vehicular
95 networks. The objective of STMAC is to support reliable
96 and fast data exchange among vehicles for driving safety via
97 the coordination of vehicular infrastructure, such as RSUs.
98 STMAC leverages a unique spatio-temporal feature to form
99 a line-of-collision (LoC) graph in which multiple vehicles
100 can transmit in the same time slot without channel inter-
101 ferences or collisions by utilizing directional antennas and
102 transmission power control. As shown in Fig. 1(a), the spatial
103 disjoint of communication areas enabled by directional anten-
104 nas provides the feature of spatial reuse, whereas the overlap
105 of the communication areas shown in Fig. 1(b) indicates

the HCF controlled channel access (HCCA) [4]. In contention-free transfer, the HCCA mechanism [4] enables the stations to transmit their QoS data to the AP according to the schedule made by the AP without any contention. On the other hand, the stations attempt to transmit their prioritized QoS data to the AP with the EDCA mechanism [4]. In both modes, the station transmits its data to its neighboring station under its communication coverage via the AP. For the purpose of driving safety, direct data delivery is possible through vehicle-to-vehicle (V2V) communication without using the data relay of an RSU. Thus, we need to design a new hybrid mode for a reliable and fast data delivery among vehicles.

Many other MAC protocols have been proposed, using MAC coordination functions (*i.e.*, DCF and PCF) to improve the efficiency and reliability of wireless media access in mobile ad hoc networks (MANETs) and vehicular ad hoc networks (VANETs). In most cases, omni-directional antenna is considered for MAC protocols even though directional antenna has several benefits. Therefore, the literature review of MAC protocols is discussed according to the coordination functions along with antenna types.

Ko *et al.* [12] propose a directional antenna MAC protocol (D-MAC) in DCF. For concurrent communications and based on D-MAC, Feng *et al.* propose a location- and mobility-aware (LMA) MAC protocol [10]. Both D-MAC and LMA perform communications in DCF mode utilizing CSMA/CA and the exponential backoff mechanism for ad hoc networks. LMA [10] is designed to achieve efficient V2V communication without infrastructure nodes (*e.g.*, RSU). The aim of LMA is to achieve efficient directional transmission while resolving the deafness problem [10]. Vehicles in LMA use the predicted location and mobility information of the target vehicle, thereby performing directed transmissions using beamforming. As an enhanced D-MAC protocol, LMA exploits the advantages of a directional antenna, such as spatial reuse, by considering the moving direction of a vehicle, and uses a longer transmission range in transmitting request-to-send (RTS), clear-to-send (CTS), data frame (DATA), and acknowledgment (ACK) as directed transmissions. However, the frame collisions increases substantially when both D-MAC and LMA are used when the vehicle density is high. This may result in a serious packet delivery delay, which is not acceptable for driving safety.

In PCF, Chung *et al.* propose a WAVE PCF MAC protocol (WPCF) [11] to improve the channel utilization and user capacity in vehicle-to-infrastructure (V2I) or infrastructure-to-vehicle (I2V) communication. The main purpose of WPCF is the dynamic reduction of the PCF interframe space (PIFS), in order to increase the channel efficiency when multiple vehicles attempt to sequentially communicate with an RSU [17]. WPCF also suggests a handover mechanism by adopting a WAVE handover controller to minimize service disconnection time [11]. However, since WPCF neither optimizes the length of a contention period (CP) nor utilizes concurrent transmissions in a contention-free period (CFP), the utilization of the wireless channel still needs to be improved. Unlike WPCF, which is a kind of HCF, STMAC allows vehicles to exchange their driving information with their neighboring

vehicles without the relaying of an RSU. Note that since WPCF is an Infrastructure-to-Vehicle (I2V) MAC protocol, the Vehicle-to-Vehicle (V2V) data delivery requires the relay via an RSU. Because this exchange is performed concurrently for the disjoint sets of vehicles, the packet delivery delay of STMAC is shorter than that of WPCF. Kim *et al.* propose a MAC protocol using a road traffic estimation for I2V communication in a highway environment [22]. Their MAC protocol estimates the road traffic to precisely control the transmission probability of vehicles in order to maximize system throughput. The protocol also presents a mechanism to use a threshold to limit the number of transmitted packets for fairness among vehicles. Hafeez *et al.* propose a distributed multichannel and mobility-aware cluster-based MAC protocol, called DMMAC [14]. DMMAC utilizes the EDCA of IEEE 802.11p to differentiate the types of packets, enables vehicles to form clusters based on a weighted stabilization factor to exchange packets.

Through the evaluation of the existing MAC protocols, we found that LMA, WPCF, and DMMAC are representatives of DCF, PCF, and cluster-based MAC protocols in VANET, respectively. Hence, the three protocols are used as baselines for performance evaluation in this paper. Comparing with LMA, WPCF, and DMMAC, STMAC leverages a spatio-temporal feature to improve the efficiency of channel access and reduce the delivery delay of safety messages. STMAC also considers an urban layout to reduce the length of the contention period. Therefore, the results will show that STMAC can outperform the legacy MAC protocols, such as LMA, WPCF, and DMMAC.

III. PROBLEM FORMULATION

The goal of the STMAC protocol is to provide a reliable and fast message exchange among adjacent vehicles through the coordination of an RSU for safe driving. To achieve this goal, a directed transmission is used whenever possible to maximize the number of concurrent transmissions through spatio-temporal transmission scheduling. The following section, we specify several assumptions and a target scenario.

A. Assumptions

The following assumptions are made in the course of designing STMAC:

- Vehicles are equipped with a DSRC interface [2] and a directional antenna array with the phase shifting [10], [23], whereas RSUs are equipped with an omnidirectional antenna. The directional antenna array can generate multiple beams toward multiple receivers at the same time (*e.g.*, MU-MIMO) [24], [25]. The narrow beam problem can be avoided in our STMAC. The direction of the each beam and the communication coverage (*i.e.*, R and β , where R is the communication range defined as a distance where a successful data frame from a sender vehicle can be transmitted to a receiver vehicle with almost no bit error, and β is the communication beam angle that is constructed by the

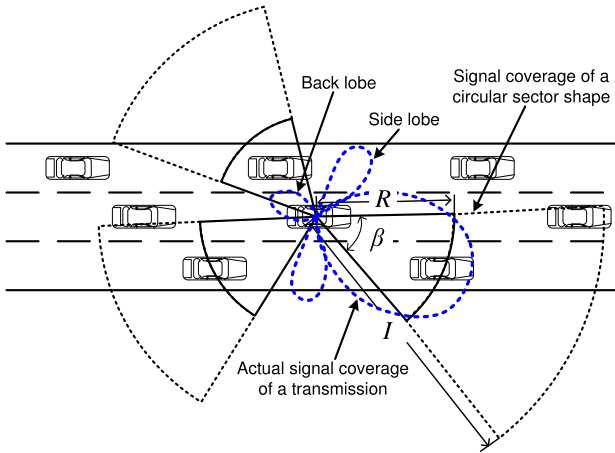


Fig. 2. A transmission signal coverage and interference range.

phase shifting of the directional antenna array [23]) are adjustable by locating the receiving vehicle's location and controlling RF transmission power [10], [23], [26], as shown in Fig. 2. The RF transmission power W_t can be determined as follows:

$$W_t = \frac{(2d)^\alpha \cdot (4\pi)^2 \cdot W_r}{\Lambda^2}, \quad (1)$$

where d is the distance between a transmitter and a receiver; α is the minimum path loss coefficient; Λ is the wavelength of a signal; W_r is the minimum power level to be able to physically receive a signal, which can be calculated by $W_r = 10^{sa/10}$, and sa is the minimum signal attenuation threshold.

- For simplicity, the interference range I of a transmission is considered to be two times the communication range R , as shown in Fig. 2, which is used in an algorithm (Algorithm 1 in Section IV-A) to decide an interference set when calculating a transmission schedule. Also, as shown in Fig. 2, a circular-sector-shape signal coverage is considered instead of the actual transmission signal coverage, and the side lobes and the back lobe are ignored for the simplicity of modeling.
- A procedure of handover similar to that of WPCF [11] is implemented in this work by using two DSRC service channels [2]. The first channel is used for the RSU's coverage, and the second channel is used for the adjacent RSU's coverage. The detailed description of the handover is given in WPCF [11].
- Vehicles are equipped with a GPS-based navigation system [19], [20]. This GPS navigation system provides vehicles with their position, speed, and direction at any time.
- The effect of buildings or trees (called terrain effect) exists in real vehicular networks. The Nakagami fading model [27] is usually used for vehicular networks. If a better fading model considering terrain effect is available, our STMAC protocol can accommodate such a model.

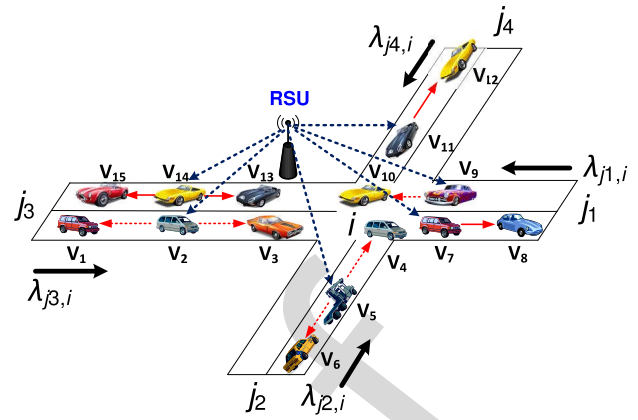


Fig. 3. The target scenario of spatio-temporal coordination by the RSU.

B. Target Scenario

Our target scenario is a vehicle data exchange, such as mobility information (e.g., location, direction, and speed) and in-vehicle device status (e.g., break, gear, engine, and axle), for driving safety in urban road networks. As shown in Fig. 3, RSUs are typically deployed at road intersections and serve as gateways between VANETs and the intelligent transportation systems (ITS) infrastructure [17]. An RSU's transmission coverage range is set to cover the maximum of the lengths of the halves of the road segments. The inter-RSU interference is avoided by letting two adjacent RSUs use different DSRC service channels. Vehicles periodically transmit time slot requests to an RSU along with their mobility information (i.e., current location, moving direction, and speed). The RSU uses the request information to construct a transmission schedule for the wireless channel access. Using the assigned time slots from the schedule, safety messages are directly exchanged between neighbor vehicles to prevent accidents. In the next section, we will explain the spatio-temporal feature and contention period optimization in STMAC protocol.

IV. SPATIO-TEMPORAL COORDINATION AND CONTENTION PERIOD OPTIMIZATION

In this section, we propose a new channel access scheme based on an enhanced set-cover algorithm by characterizing a spatio-temporal feature in urban vehicular networks. We also propose a contention period adaptation based on the vehicle arrival rate at an intersection in an urban area. To characterize the spatio-temporal feature in a vehicular environment, the formation of the line-of-collision (LoC) graph is first explained.

A. Spatio-Temporal Coordination Based Channel Access

In an urban area, a vehicle accident is usually a direct crash or collision among vehicles (e.g., frontal, side, and rear impacts). Preventing the initial direct crash can largely reduce fatalities and property losses. We propose an LoC graph among vehicles based on a geometric relation to describe the initial direct crash. As shown in Fig. 4, vehicles A and B have an LoC relation because there are no middle vehicles between them, and can therefore crash directly. From A, two tangent

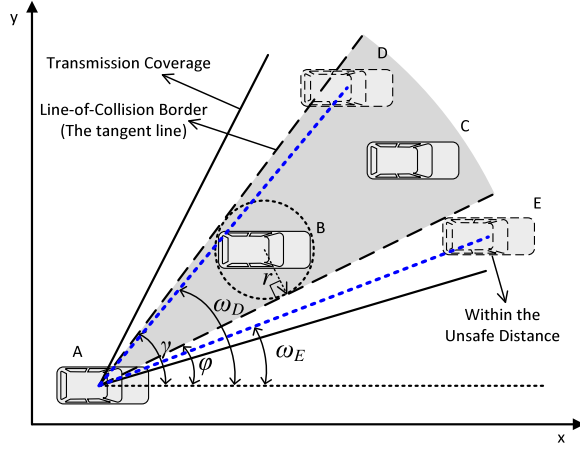


Fig. 4. Line-of-collision relation construction.

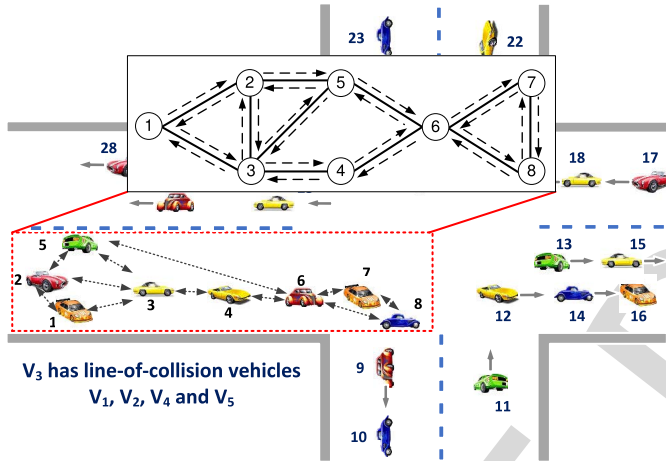
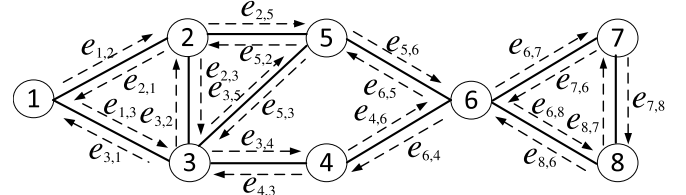


Fig. 5. Line-of-collision vehicles in road segment with multiple lanes.

349 lines on a circle can be derived based on the half length
 350 (as a radius r) of B . Any vehicle within the area between
 351 the two tangent lines (gray area in Fig. 4), but farther than
 352 B , is considered as a non-LoC vehicle to A , e.g., C in Fig. 4.
 353 By comparing the two angles γ and ϕ of the two tangent
 354 lines and the unsafe distance determined by the two-second
 355 rule [28], it can also be determined whether or not any other
 356 vehicles can be LoC vehicles of A . For example, D has no
 357 LoC relation with A because the angle ω_D is smaller than γ ,
 358 but larger than ϕ , and E is an LoC vehicle of A , based on
 359 the fact that the angle ω_E is smaller than ϕ and is within the
 360 unsafe distance. Note that vehicles with different sizes can
 361 be considered as the same class, e.g., a vehicle with a length
 362 smaller than 5 meters can be categorized as a 5 meter vehicle
 363 to determine the radius r . From communication collision point
 364 of view, if C is in the interference range of A , which is
 365 2 times transmission range of A , C can be interfered. But
 366 in our algorithm 1, this interference is avoided by scheduling
 367 vehicle A and C in different time slot, which means if C is
 368 in the interference range of A , when A is transmitting to B ,
 369 C will neither receiving nor sending a packet. Note that LoC
 370 means Line of Collision, which indicates the relationship of
 371 directly physically collision of two neighboring vehicles rather
 372 than the line-of-sight for communication range.



Start node	Edges in a time slot
3, 7	$S_1 = \{e_{3,1}, e_{3,2}, e_{3,4}, e_{3,5}, e_{7,6}, e_{7,8}\}$
2, 8	$S_2 = \{e_{2,1}, e_{2,3}, e_{2,5}, e_{8,6}, e_{8,7}\}$
1, 6	$S_3 = \{e_{1,2}, e_{1,3}, e_{6,4}, e_{6,5}, e_{6,7}, e_{6,8}\}$
5	$S_4 = \{e_{5,2}, e_{5,3}, e_{5,6}\}$
4	$S_5 = \{e_{4,3}, e_{4,6}\}$

Fig. 6. Searching sequence for maximum compatible cover-sets.

Based on the LoC relation, an LoC graph can be constructed. As shown in the dotted box of Fig. 5, we consider a scenario in which vehicles are moving in multiple lanes in road segments. The solid box in Fig. 5 shows an LoC graph $G = (V, E)$ constructed by the vehicles inside the dotted box, where the vertices in V are vehicles and the edges in E indicate an LoC relation between two adjacent vehicles that can collide directly with each other. Thus, the continuous communications are necessary for the connected vehicles in the LoC graph G . Notice that the LoC graph is used in our STMAC protocol to reduce medium collision, which is discussed in later in this section.

Through the LoC graph of the vehicles, we propose a spatio-temporal coordination based channel access scheme by using an enhanced set-cover algorithm. The enhanced set-cover algorithm for STMAC attempts to find a minimum set-cover for an optimal time slot allocation in a given LoC graph. Our STMAC Set-Cover algorithm attempts to allow as many concurrent transmissions as possible in each time slot in order to reduce the contention-free period for the required transmissions of all the LoC vehicles.

We define the following terms for the STMAC Set-Cover algorithm:

Definition 1 (Cover-Set): Let **Cover-Set** be a set S_i of edges in an LoC graph G where the edges are **mutually not interfering** (i.e., **compatible**) with each other; that is, any pair of edges $e_{u,v}, e_{x,y} \in E(G)$ are compatible with each other. For example, as shown in Fig. 6, the cover-set S_1 is $\{e_{3,1}, e_{3,2}, e_{3,4}, e_{3,5}, e_{7,6}, e_{7,8}\}$ for time slot 1.

Definition 2 (Set-Cover): Let **Set-Cover** be a set S of cover-sets S_i for $i = 1 \dots n$ that is equal to the edge set $E(G)$ such that $E(G) = \bigcup_{i=1}^n S_i$. That is, the set-cover S includes all the directed edges in an LoC graph G and represents the schedule of concurrent transmissions of the edges in S_i for time slot i . For example, Fig. 6 shows the mapping between time slot i and cover-set S_i .

We now formulate an optimization of a time slot allocation for cover-sets of non-interfering edges that can be transmitted concurrently. Let 2^N be a power set of natural number set N as time slot sets, such as $2^N = \{\emptyset, \{1\}, \{1, 2\}, \{1, 2, 3\}, \dots\}$. Let S be a set-cover for a time slot schedule. Let E be a directed edge set. Let S_i be a cover-set for a time slot i . Let $E(S_i)$

415 be the set of non-interfering edges in S_i . The optimization of
416 time slot allocation is as follows:

$$417 \quad S^* \leftarrow \arg \min_{S \in 2^N} |S|, \quad (2)$$

418 where $S = \{S_i | S_i \text{ is a cover-set for time slot } i\}$ and
419 $E = \bigcup_{S_i \in S} E(S_i)$.

420 For this optimization, we propose an STMAC Set-Cover
421 algorithm as shown in Algorithm 1. The optimization objective
422 of the STMAC Set-Cover algorithm is to *find a set-cover*
423 *with the minimum number of time slots, mapped to cover-sets*.
424 A schedule of cover-sets of which the edges are the concurrent
425 transmissions for a specific time slot can be represented as a
426 mapping from the set S of time slots S_i (i.e., cover-sets) to
427 edges $e_j \in E$. A set-cover returned as S by Algorithm 1 might
428 not be optimal since the set-covering problem is originally
429 NP-hard. That is, STMAC Set-Cover is an extension of the
430 legacy Set-Cover [21], where families (i.e., sets of elements)
431 are fixed. However, in our STMAC Set-Cover, the families are
432 not given, but should be dynamically constructed as cover-sets
433 during the mapping. Each cover-set S_i needs a time slot i ,
434 so one time slot is mapped to a cover-set that is a set of
435 non-interfering edges in G .

436 The lines 5-10 in Algorithm 1 show that the search
437 for a new maximum cover-set, which is a cover-set with
438 the maximum number of edges covered by a time slot,
439 is repeated until all the edges in E are covered by cover-
440 sets. Refer to Appendix B for the detailed description of
441 *Search_Max-Compatible_Cover_Set(G, E')* in line 6. The
442 time complexity of Algorithm 1 is $O(E \cdot V \cdot (V + E))$. Since
443 the number of vehicles at one intersection is still within a
444 reasonable bound, the time taken to calculate the optimal cover
445 set shall also be within a reasonable bound. The polynomial
446 time complexity of Algorithm 1 can be efficiently handled by
447 the edge-centric computing [18] in RSU.

Algorithm 1 STMAC-Set-Cover Algorithm

```

1: function STMAC_SET_COVER( $G$ ) ▷  $G$  is a
   line-of-collision (LoC) graph
2:  $E' \leftarrow G(E)$  ▷  $E'$  is the set of the remaining edges not
   belonging to any cover-set
3:  $S \leftarrow \emptyset$  ▷  $S$  is for a Set-Cover
4:  $i \leftarrow 1$ 
5: while  $E' \neq \emptyset$  do
6:  $S_i \leftarrow \text{Search\_Max\_Compatible\_Cover\_Set}(G, E')$ 
   ▷ search for a Maximum Cover-Set for the remaining
   edges in  $E'$ 
7:  $E' \leftarrow E' - S_i$ 
8:  $S \leftarrow S \cup \{S_i\}$ 
9:  $i \leftarrow i + 1$ 
10: end while
11: return  $S$ 
12: end function

```

448 Fig. 6 shows an example of a search sequence for a set-cover
449 with maximum cover-sets by Algorithm 1. For the first time
450 slot, in Fig. 6, vertex 3 is selected as a start node for time slot
451 1 because it has the highest degree. Vertex 7 can also transmit

452 in time slot 1 since vertex 7 is not the receiver of vertex 3
453 and has a spatial disjoint feature. Next, vertexes 2 and 8 are
454 selected as the next transmitters. Through a similar procedure
455 for the remaining vehicles, 5 time slots can cover all the
456 transmissions for the LoC graph G instead of 8 time slots
457 for each vehicle. Thus, the mapping between time slot and
458 cover-set is constructed by the STMAC Set-Cover algorithm
459 for the transmission schedule.

Note that the STMAC Set-Cover algorithm can be extended
460 to consider an interference range existing in real radio com-
461 munications [29]. Algorithm 3 in Appendix B describes
462 for the STMAC Set-Cover considering the interference
463 range.
464

B. Contention Period Optimization

465 In this section, we explain the contention period optimiza-
466 tion for the efficient channel usage, considering the arrival
467 rate of unregistered vehicles to the communication range of
468 an RSU at an intersection. This adaptation is possible because
469 vehicles in an urban area move along the confined roadways,
470 so the arrival rate can be measured in vehicular networks
471 while such a measurement is not feasible in mobile ad hoc
472 networks due to free mobility. Note that the arrival rate can
473 be measured by several ways such that loop detectors installed
474 at intersections, object recognition in traffic cameras.
475

476 The contention period is dynamically adapted according to
477 the arrival rate of unregistered vehicles to the communication
478 range of an RSU. As the number of vehicles increases for
479 an RSU, the length of CFP in the superframe duration will
480 increase, since more vehicles should be allocated with their
481 time slots for channel access. Thus, the length of CP should
482 be determined according to the expected number of arriving,
483 unregistered vehicles in one superframe duration to enable the
484 vehicles the opportunity to be registered in the RSU with a
485 registration frame. If the CP length is too short, registration
486 frames toward the RSU will encounter many collisions during
487 registration attempts, and only a few vehicles can therefore
488 be registered. In contrast, if the CP length is too long, most
489 of the time in CP will be wasted after registering all arriving
490 vehicles in the RSU, resulting in a poor channel utilization.
491 Thus, we need to find the appropriate length of CP to guarantee
492 new incoming vehicles are given the opportunity to registered
493 with the RSU in a finite period of time (e.g., one superframe
494 duration) within the same superframe.

495 Let λ_{jki} denote the vehicle arrival rate from an adjacent
496 intersection j_k to an intersection i , as shown in Fig. 3. Let λ
497 be the total arrival rate for the communication range of RSU
498 at intersection i per unit time (e.g., 1 second) such that

$$499 \quad \lambda = \sum_{k=1}^n \lambda_{jki}. \quad (3)$$

500 Here n is the number of neighbor intersections of inter-
501 section i . RSU at an intersection i observes the number of
502 vehicles that arrive within its transmission coverage from its
503 adjacent road segments. We can simply calculate λ with the
504 total arrivals of vehicles for all incoming road segments per
505 unit time.

We leverage the concept of the slotted ALOHA [30] and the Reservation-ALOHA (R-ALOHA) [31] for CP adaptation. The original R-ALOHA was designed for ad hoc networks to reduce collisions [32], whereas the CP in our scheme is designed for vehicle registration to reserve time slots in the next CFP. R-ALOHA provides nodes with time-based multiple channel access in a wireless link with a reasonable access efficiency (i.e., channel utilization) [31]. In CP, since new comer vehicles to an intersection area try to register their mobility information into the RSU with a single registration frame, R-ALOHA can be used for the CP in STMAC. Let s be the time duration of one superframe duration including CP and CFP duration.

- An unregistered vehicle attempts to send its registration frame with probability p .
- N vehicles attempt to be registered in RSU in this superframe duration, such that $N = \lambda \cdot s$.
- The probability that one vehicle succeeds in registering its transmission request for a slot among N vehicles is:

$$g_N = N \cdot p \cdot (1 - p)^{N-1}. \quad (4)$$

For the CP duration, the total number of slots to register N vehicles is:

$$M = \sum_{i=N}^1 \frac{1}{g_i} = \sum_{i=N}^1 \frac{1}{i \cdot p \cdot (1 - p)^{i-1}}. \quad (5)$$

Appendix A provides the detailed derivation for this equation. For the efficient operation, the possible values of λ are mapped into a pair of the optimal channel access probability p and total slot number M in off-line processing. This pair of p and M for the current λ is announced to unregistered vehicles by an RSU through a timing advertisement frame (TAF), specified in Section V. Note that although the RSUs are responsible for the vehicle registration and the cover-set calculations, they can handle these procedures because each RSU only manages one intersection at which the number of vehicles is still bounded to a reasonable level, even in rush-hours.

So far, we have described the proposed spatio-temporal coordination-based channel access scheme and the contention period optimization. In the next section, we will introduce a new hybrid MAC protocol to combine the merits of PCF and DCF modes based on the proposed channel access scheme and the contention period optimization.

V. SPATIO-TEMPORAL COORDINATION BASED MEDIA ACCESS CONTROL PROTOCOL

STMAC is a hybrid MAC protocol that combines the PCF and DCF modes for efficient channel utilization and quick driving safety information exchange. The PCF mode is used to (i) register unregistered vehicles in an RSU with their mobility information, (ii) construct a collision-free channel access schedule for registered vehicles, and (iii) announce the channel access schedule for V2V communications in a similar way to that of WPCF [11]. In contrast, the DCF mode is used to enable the safety messages of the registered vehicles to be exchanged with other registered vehicles and without frame collision in V2V communications.

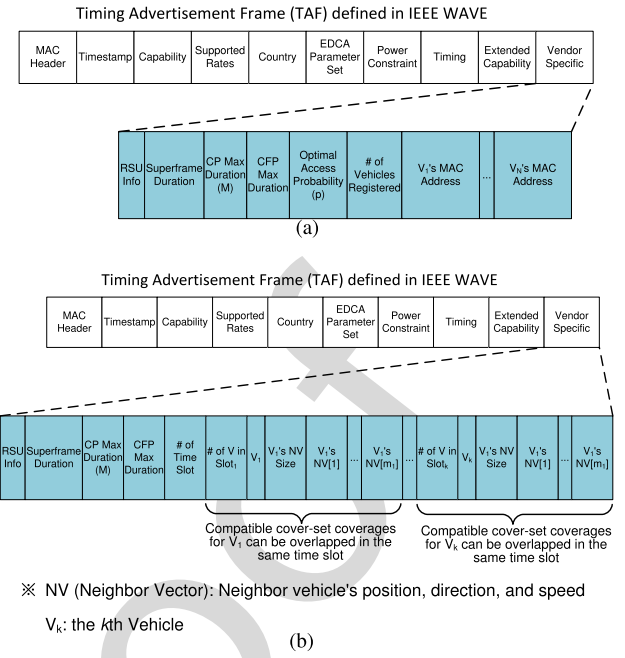


Fig. 7. Timing advertisement frame (TAF) formats in STMAC. (a) TAF in CP. (b) TAF in CFP.

In STMAC, an RSU periodically broadcasts a timing advertisement frame (TAF). The TAF is a beacon frame following the standard of the IEEE WAVE [33]. In STMAC, it has two formats, including TAF in CP and TAF in CFP as shown in Fig. 7. Both formats in the vendor specific field have some common fields, such as RSU information, superframe duration, CP max duration (i.e., M), and CFP max duration. The vendor specific field of TAF for CP shown in Fig. 7(a) additionally contains optimal access probability (i.e., p), the number of vehicles registered, and registered vehicles' MAC addresses. The vendor specific field of TAF for CFP in Fig. 7(b) contains other information, such as the number of time slots, the transmission schedule in each time slot, and the neighbor vectors (NV). NV contains the mobility information (i.e., the current position, direction, and speed) of neighboring vehicles.

In STMAC, time is divided into superframe duration, and each superframe duration consists of two phases, the CP phase and CFP phase, as shown in Fig. 8. These two phases are explained in the following subsections.

A. CP Phase for Vehicle Registration

In the CP phase, unregistered vehicles attempt to be registered in an RSU based on contention. Fig. 8(a) shows a contention-period time sequence for vehicle registration. As shown in Fig. 8(a), a TAF at the beginning of a CP is firstly transmitted by an RSU in a DSRC control channel (CCH), after a DCF inter frame space (DIFS) period, indicating the start of a contention period.

The TAF mainly contains a list of the registered vehicles and the RSU's service channel number (SCH#) in the RSU Info part as shown in Fig. 7(a). Next, after receiving the TAF, the vehicles start contending the transmission opportunity to send a registration request (i.e., REQ in Fig. 8(a)). It is possible

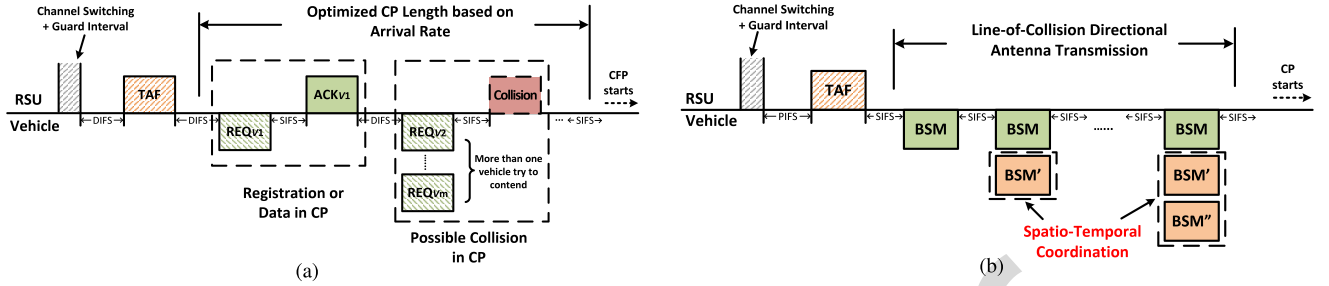


Fig. 8. Time sequence in STMAC protocol. (a) Contention-period time sequence. (b) Contention-free-period time sequence.

591 that multiple vehicles attempt to contend, causing a collision
 592 at the RSU. After this contention period, the contention free
 593 period starts and all registered vehicles (including newly reg-
 594 istered vehicles) switch their CCH channel to an SCH channel
 595 specified in the TAF.

596 Let O_c be the number of vehicles that send packets, then
 597 the maximum CP length can be calculated as follows:

$$598 T_{CP}^{STMAC} = DIFS + TAF + (DIFS + REQ + SIFS + ACK) \\
 599 \cdot \sum_{i=0}^{O_c} \frac{1}{i \cdot p \cdot (1-p)^{i-1}} + SIFS + T_{CS} + T_{GI}, \quad (6)$$

600 where $DIFS$, TAF , REQ , $SIFS$, ACK , T_{CS} , and T_{GI} are
 601 the time for the DCF inter frame space, the timing adver-
 602 tisement frame, the registration request frame, the short inter
 603 frame space, the acknowledgement frame, the channel switch,
 604 and the guard interval, respectively, and $\sum_{i=0}^{O_c} \frac{1}{i \cdot p \cdot (1-p)^{i-1}}$
 605 is the expected number of vehicle registrations derived
 606 in Section IV-B.

607 Note that during the CP phase, both registered and unregis-
 608 tered vehicles can transmit an emergency message to an RSU
 609 for emergency data dissemination (e.g., an accident).

611 B. CFP Phase for Driving Information Exchange

612 In a CFP phase, registered vehicles attempt exchange their
 613 driving safety information with their neighboring vehicles
 614 based on the contention-free schedule in service chan-
 615 nels (SCHs). As shown in Fig. 8(b), a TAF containing the
 616 channel access schedule of registered vehicles is broadcasted
 617 by an RSU. Each vehicle based on the schedule in the TAF
 618 transmits its basic safety message (BSM) (e.g., mobility infor-
 619 mation and vehicle internal states) to its intended receivers for
 620 the time slot. As shown in the dashed line box of Fig. 8(b),
 621 the transmissions of BSM packets are multiplexed in the time
 622 slots according to the spatio-temporal coordination described
 623 in Section IV-A. Let O_r^{STMAC} be the number of time slots
 624 allocated by the spatio-temporal coordination in a CFP; then,
 625 O_c vehicles may use O_r^{STMAC} time slots to exchange safety
 626 messages. Thus, the maximum length of a CFP in STMAC
 627 can be expressed as:

$$628 T_{CFP}^{STMAC} = PIFS + TAF + \sum_{i=1}^{O_r^{STMAC}} (SIFS + BSM_i) \\
 629 + SIFS + T_{CS} + T_{GI}, \quad (7)$$

630 where $PIFS$ and BSM_i are the time for the PCF interframe
 631 space and the basic safety message for vehicle i , respectively.

632 Using the NVs from the TAF, each vehicle i constructs the
 633 coverage regions for its intended transmissions by the direc-
 634 tional antenna and the transmission power control. Note that
 635 during the CFP phase, if the RSU has an emergency message,
 636 it can announce a TAF having emergency information.

637 Thus, by the CP and CFP phases, STMAC can allow for
 638 not only the fast exchange of driving safety information among
 639 vehicles, but also the fast dissemination of emergency data of
 640 the vehicles under the RSU.

641 C. Vehicle Mobility Information Update

642 In the STMAC protocol, the RSU periodically broadcasts
 643 a special TAF in a CP phase to collect the most current
 644 mobility information of all registered vehicles. This enables
 645 vehicles to correctly select the transmission direction and
 646 power control parameters by the latest position of a receiver
 647 vehicle. This TAF is also used to deregister vehicles that
 648 have left the communication range of the RSU, and which
 649 do not respond to this TAF. Each registered vehicle sends
 650 its updated mobility by transmitting a BSM, which includes
 651 its mobility information, to the RSU. The superframe for the
 652 vehicle mobility information update is repeated every U times,
 653 such as $U = 10$, considering the mobility prediction accuracy.
 654 With this update, the RSU estimates the vehicle's mobility
 655 in the near future (e.g., after 100 milliseconds) for time slot
 656 scheduling.

657 D. Performance Analysis

658 We have so far explained the design of STMAC protocol.
 659 Now we analyze the performance of STMAC and WPCF.
 660 Since WPCF is the MAC protocol most similar to STMAC,
 661 we particularly study the performance of WPCF. Table I
 662 shows the performance analysis of STMAC and WPCF. The
 663 maximum CP and CFP lengths of STMAC were discussed
 664 in Sections V-A and V-B. Notice that the number of time
 665 slots (i.e., O_r^{STMAC}) allocated in a CFP of STMAC is a result
 666 of the spatio-temporal coordination. The acknowledgement
 667 process between any two LoC vehicles, of which the time
 668 is $SIFS + ACK$, is removed to improve the efficiency of the
 669 safety information exchange. We assume that every vehicle has
 670 safety messages that must be sent. The superframe duration
 671 of STMAC can be described as

$$672 T_{SF}^{STMAC} = T_{CP}^{STMAC} + T_{CFP}^{STMAC}. \quad (8)$$

TABLE I
 PERFORMANCE ANALYSIS OF STMAC AND WPCF

Scheme	Maximum CP Length (T_{CP})	Maximum CFP Length (T_{CFP})
STMAC	$DIFS + TAF + (DIFS + REQ + SIFS + ACK) \cdot \sum_{i=O_c}^1 \frac{1}{i \cdot p \cdot (1-p)^{i-1}} + SIFS + T_{CS} + T_{GI}$	$PIFS + TAF + \sum_{i=1}^{O_r^{STMAC}} (SIFS + BSM_i) + SIFS + T_{CS} + T_{GI}$
WPCF [11]	$DIFS + TAF + (DIFS + REQ + SIFS + ACK) \cdot \sum_{i=O_c}^1 \frac{1}{i \cdot p \cdot (1-p)^{i-1}} + SIFS + END$	$SIFS + TAF + \sum_{i=1}^{O_r} (WPIFS[1] + BSM_i + SIFS + ACK) + END$

673 The maximum CP length T_{CP}^{WPCF} of WPCF is similar to
 674 that of STMAC, but WPCF has no registration mechanism
 675 for continuous communications, which means that whenever
 676 a vehicle has a packet to send, it needs to reserve a time slot
 677 in a CP. Also, the vehicles with the WPCF scheme, which
 678 reserved the time slots in the CP, do not utilize the spatial
 679 feature to reduce the number of time slots. Thus, the maximum
 680 CFP length of WPCF is determined by the number of vehicles
 681 with reserved time slots in the CP. Note that the number of
 682 vehicles within the coverage of one RSU at an intersection is
 683 a reasonable number, the CFP period will increase reasonably
 684 as the number of vehicles increases. Assume that there are O_r
 685 vehicles having packets to send; the maximum CFP length for
 686 these O_r vehicles is:

$$687 T_{CFP}^{WPCF} = SIFS + TAF + \sum_{i=1}^{O_r} \times (WPIFS[1] + BSM_i + SIFS + ACK) + END, \quad (9)$$

690 where $WPIFS$ is the WAVE PCF inter frame space defined
 691 in WPCF [11]; $WPIFS[k] = SIFS + (k \times T_{slot})$; k is the
 692 sequence number for the transmission order of a vehicle in the
 693 current CFP schedule, and k is always 1 because every reg-
 694 istered vehicle transmits its data frame to the RSU according
 695 to its transmission order in the schedule [11]; BSM_i is the
 696 transmission time of the basic safety message for a vehicle i ;
 697 and END is the CFP end frame sent by an RSU, which can
 698 be equal to the $T_{CS} + T_{GI}$ of STMAC. Thus, the superframe
 699 duration T_{SF}^{WPCF} of WPCF is

$$700 T_{SF}^{WPCF} = T_{CP}^{WPCF} + T_{CFP}^{WPCF}. \quad (10)$$

701 To measure the interval between two consecutive safety
 702 messages which are transmitted by a vehicle and are received
 703 by its neighboring vehicles, we define E2E delay to describe
 704 it. Based on the superframe duration of STMAC and WPCF,
 705 the E2E delay of STMAC (denoted as T_{E2E}^{STMAC}) and that of
 706 WPCF (denoted as T_{E2E}^{WPCF}) can be estimated by the uniformly
 707 distributed channel access in both CP and CFP phases:

$$708 T_{E2E}^{STMAC} = \frac{T_{CFP}^{STMAC}}{2} + T_{CP}^{STMAC} + \frac{T_{CP}^{STMAC}}{2}$$

$$709 = \frac{T_{SF}^{STMAC}}{2} + T_{CP}^{STMAC}. \quad (11)$$

$$710 T_{E2E}^{WPCF} = \frac{T_{CFP}^{WPCF}}{2} + T_{CP}^{WPCF} + \frac{T_{CP}^{WPCF}}{2}$$

$$711 = \frac{T_{SF}^{WPCF}}{2} + T_{CP}^{WPCF}. \quad (12)$$

 TABLE II
 PARAMETERS FOR PERFORMANCE ANALYSIS

Parameter	Value
T_{slot}	13 μs
SIFS	32 μs
PIFS	45 μs (SIFS + T_{slot})
DIFS	58 μs (SIFS + $T_{slot} \times 2$)
$T_{CS} + T_{GI}$ (END)	4 ms
Data rate	6 Mbps
Size of TAF packet	800 bit + Payload
Size of BSM packet	1024 bit + 88 bit
Size of REQ packet	288 bit
Size of ACK packet	128 bit

712 We verified the analytical models of STMAC and WPCF
 713 by comparing the analytical results with the simulation results
 714 in Section VI-B based on the parameters in Table II. Note that
 715 the contents of a BSM can be modified to adapt to different
 716 scenarios, which may vary the size of a BSM.

717 Since it is a CSMA/CA-based MAC scheme, LMA does
 718 not have the concept of superframe. Thus, we cannot deter-
 719 mine the superframe duration as we can for STMAC and
 720 WPCF. Note that many analysis models have been proposed
 721 (e.g., Markov chain model [34]–[37]) to describe the perfor-
 722 mance of CSMA/CA schemes.

723 So far, we have explained the design of the STMAC
 724 protocol. In the next section, we will evaluate our STMAC
 725 with baselines in realistic settings.

726 VI. PERFORMANCE EVALUATION

727 In this section, we evaluate the performance of STMAC
 728 in terms of average superframe duration, E2E delay, and
 729 packet loss ratio as performance metrics. We set the data
 730 rate as 6 Mbps, and utilize the Nakagami-3 [27] radio model
 731 for both transmitter and receiver to support the irregularity of
 732 transmission coverage, interference, and path loss in vehicular
 733 environments. We assume that a transmission coverage can be
 734 optimized in STMAC from a design perspective for an opti-
 735 mized communication coverage. Also, multiple transmissions
 736 can be emitted toward multiple receivers by a transmitter's
 737 directional antenna.

738 The evaluation settings are as follows:

- 739 • **Performance Metrics:** We use (i) *Average superframe*
 740 *duration*, (ii) *E2E delay*, and (iii) *Packet loss ratio* as
 741 metrics for the performance.
- 742 • **Baseline:** LMA [10], WPCF [11], DMMAC [14], and
 743 EDCA [4] were used as baselines.

TABLE III
SIMULATION CONFIGURATION

Parameter	Description
Road network	The number of intersections is 11. The area of the road map is $500 \text{ m} \times 600 \text{ m}$ (<i>i.e.</i> , $0.31 \text{ miles} \times 0.37 \text{ miles}$).
Number of vehicles (N)	The number of vehicles moving in the road network ranges from 50 to 300. The default is 150.
Communication range (R)	$R = 25 \sim 150$ meters (<i>i.e.</i> , $82.02 \sim 492.13$ feet). The default is 75 meters.
GPS location error (ϵ)	$\epsilon = 0 \sim 18$ meters (<i>i.e.</i> , $0 \sim 59$ feet). The default is 3 meters.
Maximum vehicle speed (v_{max})	Maximum vehicle speed (<i>i.e.</i> , speed limit) for road segments. The default is 22.22 m/s (<i>i.e.</i> , 49.7 MPH).
Radio delay (d_r)	The time taken to switch from Rx to Tx mode for OFDM PHY defined in IEEE 802.11-2012 [4]. The default is $1 \mu\text{s}$.
Transmission power (P)	The value is variable, decided by equation (1) and Algorithm 1
Data traffic rate	The frequency of safety information transmission. The default is 100 packets per second.

- 744 • **Parameters:** For the performance, we investigate the
745 impacts of the following parameters: (i) *Vehicle num-*
746 *ber* (*i.e.*, Vehicle traffic density) N , (ii) *GPS position*
747 *error* (*i.e.*, Vehicle location error) ϵ , (iii) *Radio antenna,*
748 *and* (iv) *Contention period duration.*

749 We use a road network with 11 intersections associated with
750 11 RSUs from a rectangular area of Los Angeles, CA, U.S.A.
751 using Open Street Map [38] as shown in Fig. 9. The total
752 length of the road segments of the road network is about
753 4.92 km (*i.e.*, 3.06 miles). We built STMAC, WPCF, LMA,
754 and DMMAC using OMNeT++ [39] and Veins [40] as well
755 as applying the settings specified in Table III. Veins is an
756 open source software to simulate vehicle communication and
757 networks, including signal fading models. Directional antenna
758 coverage is formed by a directional antenna array [23] on
759 top of a realistic wireless radio model in Veins, such as
760 Nakagami fading model [27]. To use realistic vehicle mobility
761 in the road network, we fed the vehicle mobility information
762 to OMNeT++ using a vehicle mobility simulator called
763 SUMO [41] via the TraCI protocol [41]. SUMO was extended
764 such that vehicles move around, rather than escape from a
765 target road network.

766 Because our objective is to show the performance of local
767 communications among RSU and vehicles in the same road
768 segment, rather than the E2E delivery delay between two
769 remote vehicles in a large-scale road network, the simulation
770 topology shown in Fig. 9 is sufficient for evaluating our
771 proposed protocol. The packets for safety messages continue
772 to be generated during the travel of vehicles. We averaged
773 10 samples with confidence interval (*i.e.*, error bar) in the
774 performance results.

775 A. Comparison of Data Delivery Behaviors

776 We compared the data delivery behaviors of STMAC,
777 WPCF, LMA, DMMAC, and EDCA with the cumulative
778 distribution function (CDF) of the superframe duration,

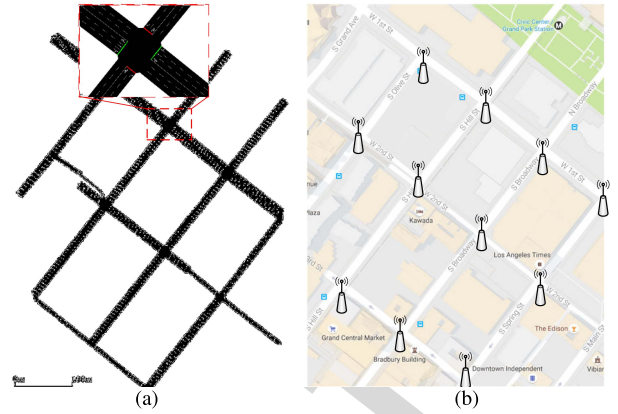


Fig. 9. Road network for simulation. (a) Extracted map in SUMO. (b) Real map with RSU placement.

779 E2E delay, and packet loss ratio. Fig. 10 shows that the
780 CDF of STMAC reaches 100% much faster than those of
781 WPCF, LMA, DMMAC, and EDCA. For example, STMAC
782 has the average superframe duration of 0.021 s for 80% CDF,
783 while for the same CDF value, WPCF has that of 0.052 s .
784 Also, STMAC has the E2E delay of 0.017 s for 80%
785 CDF while WPCF has that of 0.055 s and LMA has that
786 of 1.2 s . In addition, The packet loss ratio of STMAC
787 is 0.3% for 80% CDF. While that for WPCF is 25% and
788 that for LMA is 1.8%. We observed that STMAC has better
789 channel utilization, shorter E2E delay, and less packet loss
790 ratio than WPCF, LMA, DMMAC, and EDCA. We show the
791 forwarding performance of these three schemes quantitatively
792 in the following subsections.

793 B. Impact of Number of Vehicles

794 To examine the impact of the vehicle density, we varied the
795 number of vehicles from 50 to 300 in the simulations. Since
796 LMA, DMMAC, and EDCA do not have a superframe period,
797 we only verified the analytical results of superframe duration
798 and E2E delay of STMAC and WPCF.

799 Fig. 11(a) shows both the analytical and simulation results
800 of the average superframe duration for the different vehicle
801 densities. We obtained the analytical results from the analysis
802 in Section V-D by uniformly assigning vehicles to each RSU.
803 Note that the setting of uniformly distributed vehicles is used
804 to get the performance results of the theoretical analysis in
805 Section V-D. In the simulation, the vehicles are not uniformly
806 distributed. The vehicle traffic is from SUMO which models a
807 realistic vehicle mobility. Vehicles select their random destina-
808 tion and move to the destination in a shortest path. The results
809 in Fig. 11(a) show that the simulation data match well with the
810 analytical results. The average superframe duration of STMAC
811 is shorter than that of WPCF. Especially, in a highly congested
812 road situation, STMAC outperforms WPCF by 66.7%. It was
813 observed that when the vehicle density increases, a small gap
814 appears between the simulation and the analytical data of
815 WPCF. This is due to the non-uniform vehicle distribution
816 in the simulation. A small gap between the simulation result
817 and analytical result of STMAC is also observed, but due to

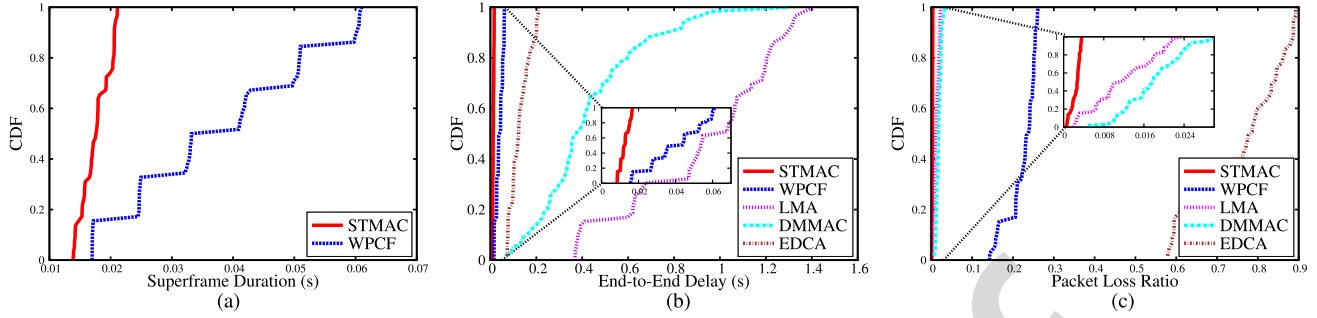


Fig. 10. CDF of superframe duration, E2E delay and packet loss ratio for STMAC, WPCF, and LMA. (a) CDF of superframe duration. (b) CDF of E2E delay. (c) CDF of packet loss ratio.

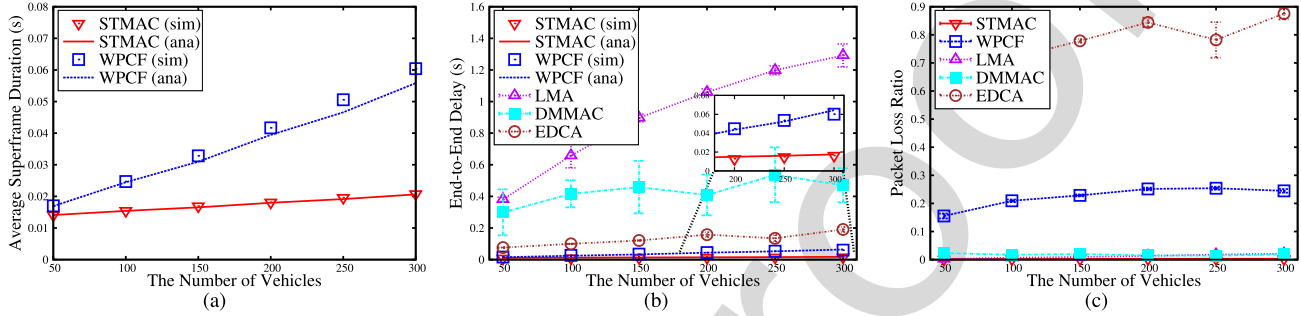


Fig. 11. Impact of the number of vehicles. (a) Average superframe duration for STMAC and WPCF. (b) Packet E2E delay for STMAC, WPCF, and LMA. (c) Packet loss ratio for STMAC, WPCF, and LMA.

818 the scale of the figure, such a gap is not significant. Notice
 819 that in Fig. 11(a), the curve of STMAC is linearly increasing
 820 rather than constant according to the increase of vehicles.
 821 Also, note that the average superframe duration determines
 822 the time duration of a vehicles safety information transmission
 823 toward its adjacent vehicles in the LoC graph. Thus, the shorter
 824 average superframe duration indicates the more often exchange
 825 of safety information among vehicles.

826 As described in Section V-D, the average superframe duration
 827 determines the packet E2E delay. Fig. 11(b) shows the
 828 analytical and simulation results of the average E2E delay of
 829 packet delivery. Overall, the simulation results show a good
 830 agreement with the analytical results, as shown in the small
 831 window of Fig. 11(b). As the number of vehicles increases,
 832 all of STMAC, WPCF, LMA, DMMAC, and EDCA have
 833 a longer average E2E delay. In any road traffic condition
 834 (*i.e.*, $N = 50$ through $N = 300$), STMAC has a shorter packet
 835 E2E delay than WPCF, LMA, DMMAC, and EDCA due to
 836 both the optimized CP duration and concurrent transmissions
 837 by spatio-temporal coordination. Especially, for highly con-
 838 gested road traffic of $N = 300$, the packet E2E delay of
 839 STMAC is one third that of WPCF. Notice that the E2E
 840 delay of LMA is identical to that in the results reported in
 841 LMA [10]. LMA has much higher E2E delays than those of
 842 STMAC and WPCF in all vehicle densities. This is due to the
 843 mechanism of Carrier Sense Multiple Access with Collision
 844 Avoidance (CSMA/CA) [4] that can let multiple control frames
 845 experience collision before the transmission of a data frame.

846 Fig. 11(c) shows the packet loss ratio according to the
 847 increasing number of vehicles. In all vehicle densities from

50 to 300, STMAC has a much lower packet loss ratio than
 both WPCF, LMA, DMMAC, and EDCA since in STMAC,
 vehicles can communicate with their LoC vehicles by an
 optimized communication range. Even for highly congested
 road traffic of $N = 300$, STMAC gains a packet loss ratio less
 than 1%, but for the packet loss ratio of WPCF and LMA are
 24% and 2.5%, respectively. Through the observation of the
 simulations, the high packet loss ratio of WPCF is caused by
 signal attenuation and the packet collisions in handover areas.
 The packet loss of LMA, which lacks spatial coordination,
 is produced mainly by the packet collisions between the data
 frames and the control frames. The spatial coordination and
 the transmission power control induce a very low packet loss
 ratio for STMAC.

848 From the performance comparison of the superframe duration,
 849 the E2E delay, and the packet loss ratio, STMAC
 850 outperforms the other state-of-the-art schemes considerably,
 851 indicating that it can support reliable and fast safety message
 852 exchange. These improvements are because that STMAC
 853 allows vehicles to transmit their safety information frames
 854 with their neighboring vehicles in the LoC graph through
 855 spatio-temporal coordination in an RSU in a direct V2V com-
 856 munication. This coordination can reduce the frame collision
 857 and the direct V2V communication reduces the data delivery
 858 between vehicles. On the other hand, LMA lets vehicles
 859 access the wireless channel randomly, so this increases the
 860 frame collision probability as the number of vehicles increases.
 861 Also, since WPCF does not consider CP duration optimization
 862 unlike STMAC, the channel utilization of WPCF is worse than
 863 that of STMAC.
 864
 865
 866
 867
 868
 869
 870
 871
 872
 873
 874
 875
 876
 877

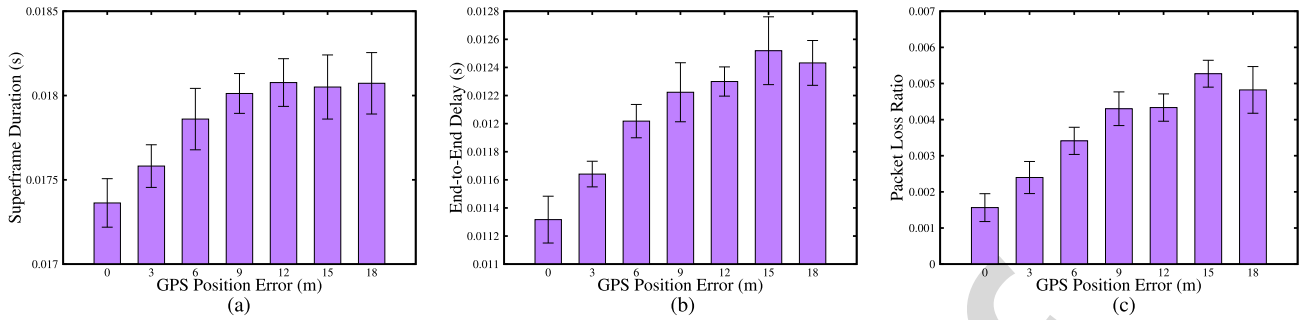


Fig. 12. Impact of GPS position error. (a) Average superframe duration. (b) Packet E2E delay. (c) Packet loss ratio.

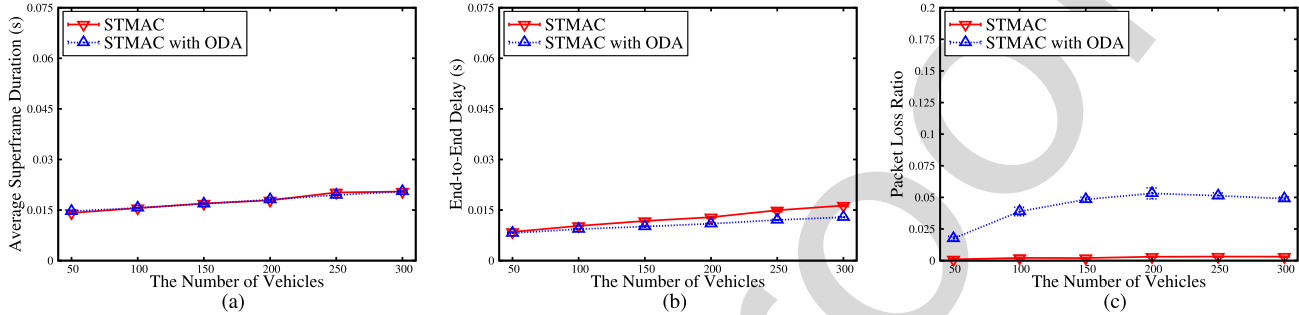


Fig. 13. Impact of radio antenna. (a) Average superframe duration with omni-directional antenna. (b) Packet E2E delay with omni-directional antenna. (c) Packet loss ratio with omni-directional antenna.

C. Impact of GPS Position Error

In an urban area, tall buildings usually seriously affect the precision of GPS localization, which can also influence the performance of STMAC since STMAC utilizes the coordinates of vehicles to schedule time slots. Therefore, we evaluated the performance of STMAC by varying the GPS position error at a medium vehicle density (*i.e.*, 150 vehicles). Fig. 12 shows the average superframe duration, E2E delay, and packet loss ratio according to GPS position error. The average superframe duration of STMAC increases when the GPS error increases, as shown in Fig. 12(a), but when the error reaches above 9 meters, the average superframe duration remains stable. The worst case occurred at the GPS position error with 12 meters, where the average superframe duration is about 18.1 ms, which is still within a safe driving range (*e.g.*, 100 ms [42]). On the other hand, as the GPS error increases, the E2E delay also increases as shown in Fig. 12(b), and the worst case is about 12.5 ms on average. For packet loss ratio, in the zero GPS position error, STMAC performs with less than 0.18% packet loss ratio, and gains increased packet loss ratio as the GPS error range increases. From the result shown in this figure, it is expected that STMAC can work well for safety message exchange [42] even in urban road networks with a high GPS error due to buildings. The good tolerance of GPS error in STMAC benefits from the design of STMAC protocol. Algorithm 1 considers the GPS error when using the vehicles position information to schedule the transmissions. Based on the algorithm, vehicles transmit data following the enlarged transmission range to compensate the impact of GPS error.

D. Impact of Radio Antenna

To evaluate the impact of radio antenna, we conducted simulations by switching the radio antenna. Fig. 13 shows the impact of radio antenna, such as directional antenna and omni-directional antenna (ODA). As shown in Fig. 13(a), STMAC using directional antenna has almost the same superframe duration as that of STMAC using ODA. For packet E2E delay, as shown in Fig. 13(b), STMAC using directional antenna has slightly longer E2E delay than STMAC using ODA. This is because vehicles using ODA in STMAC exchange safety messages with adjacent vehicles when updating their mobility information to RSUs; this update reduces the E2E delay of safety messages.

For data packet loss ratio, as shown in Fig. 13(c), the data packet loss ratio of STMAC when using the directional antenna is less than that of STMAC when using ODA. The data packet loss when using ODA is due to two factors: signal attenuation and the packet loss in handover areas. The packet loss in handover areas results from the channel switch of vehicles in the handover areas. Assume that vehicle A (V_A) that is moving into a handover area becomes registered in a new RSU (RSU_n) and its service channel is switched according to RSU_n . The predecessor RSU (RSU_p) of V_A can still generate transmission schedules including V_A until the next update period. The other vehicles in RSU_p receiving the schedules can transmit their data packets to V_A in the handover area, although V_A has switched from the service channel of RSU_p to the service channel of RSU_n . The vehicles with ODA in RSU_p can increase the data packet loss in the handover areas, since V_A in the handover area can receive

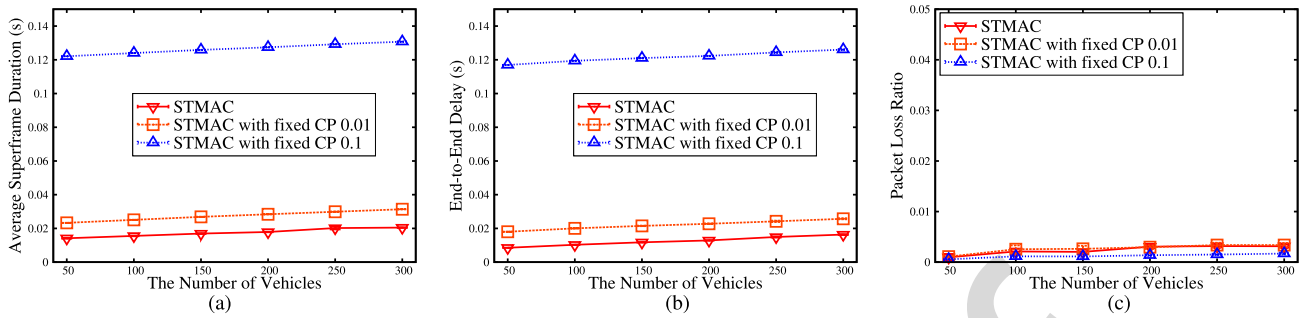


Fig. 14. Impact of contention period duration. (a) Average superframe duration for CP duration. (b) Packet E2E delay for CP duration. (c) Packet loss ratio for CP duration.

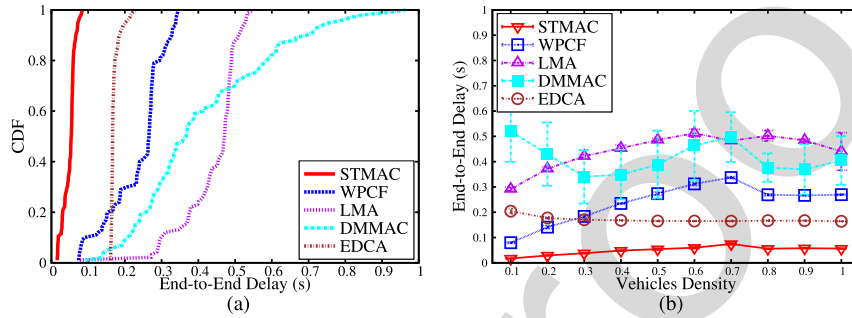


Fig. 15. Performance in highly congested scenario. (a) CDF of E2E delay at one intersection. (b) Packet E2E delay at one intersection.

938 more data packets from the vehicles with ODA than from the
 939 vehicles with directional antenna. However, this data packet
 940 loss does not affect the average packet E2E delay, because the
 941 vehicles in handover areas can receive data packet correctly
 942 from the other vehicles in the coverage of RSU_n , as shown
 943 in Fig. 13(b).

944 The results in Fig. 13 indicate that STMAC with directional
 945 antenna can significantly reduce packet loss while maintaining
 946 a good packet E2E delay in comparison with STMAC with
 947 omni-directional antenna.

948 *E. Impact of Contention Period Duration*

949 We also fixed the length of the CP to show the impact of
 950 the contention period duration. Particularly, we select 100 ms
 951 and 10 ms for the fixed-length CP to evaluate the performance
 952 of STMAC with the CP adaptation. Fig. 14 shows the impact
 953 of CP duration in STMAC. For average superframe duration,
 954 as shown in Fig. 14(a), the E2E delay of STMAC with
 955 CP adaptation has shorter average superframe duration than
 956 STMAC with constant CP duration (*i.e.*, 0.01s and 0.1 s,
 957 respectively). For packet E2E delay with CP adaptation,
 958 as shown in Fig. 14(b), the E2E delay of STMAC with CP
 959 adaptation is shorter than STMAC with both constant CP
 960 durations. For packet loss ratio with CP adaptation, as shown
 961 in Fig. 14(c), STMAC has small packet loss regardless of
 962 CP adaptation. This small packet loss ratio benefits from the
 963 directional antenna that reduces packet collisions.

964 *F. Performance in Highly Congested Scenario*

965 To measure the scalability of STMAC, we performed a
 966 simulation in a highly congested scenario at one intersection

with four road segments. The intersection has three lanes 967
 on each road segment, and the length of each road seg- 968
 ment is 300 meters. An RSU is placed at the intersection. 969
 Consider a vehicle with 5 meters length, and the minimum 970
 gap between two vehicles is 2.5 meters. To fully occupy the 971
 intersection, about 922 vehicles are required at the intersection. 972
 Fig. 15 shows the E2E delay performance among STMAC, 973
 WPCF, LMA, DMMAC, and EDCA. STMAC obtained the 974
 best performance on the E2E delay, which shows that the 975
 scalability of STMAC is good. In Fig. 15(a), the packet E2E 976
 delays in STMAC are always within 100 ms even in the full 977
 congested scenario, which can fulfill the minimum requirement 978
 for driving safety information exchange. Fig. 15(b) shows the 979
 trend of the packet E2E delay from a low density to a high 980
 density. With the increase of vehicles density, the packet E2E 981
 delays in STMAC, WPCF, and LMA also increase. The packet 982
 E2E delay in STMAC is much lower than that of WPCF and 983
 LMA, which is gained by the enhanced set-cover algorithm 984
 and the new hybrid MAC protocol utilizing the spatio-temporal 985
 coordination. Also, notice that the E2E delays in STMAC 986
 and WPCF reach the highest point at the vehicles density 987
 with 0.7. After the peak, the E2E delay maintains as almost 988
 constant. Based on the observation, the peak indicates the 989
 saturation scenario within the coverage of the RSU. When 990
 vehicles density is larger than 0.7, the intersection experiences 991
 traffic jam that hinders vehicles to move into the coverage of 992
 the RSU, which reduces the E2E delay. 993

Therefore, the results from the performance evaluation show 994
 that STMAC is a promising MAC protocol for driving safety 995
 to support the reliable and rapid exchange of safety messages 996
 among nearby vehicles. 997

VII. CONCLUSION

In this paper, we propose a Spatio-Temporal Coordination based Media Access Control (STMAC) protocol in an urban area for an optimized wireless channel access. We characterize the spatio-temporal feature using a line-of-collision (LoC) graph. With this spatio-temporal coordination, STMAC organizes vehicles that transmit safety messages to their neighboring vehicles reliably and rapidly. Vehicles access wireless channels in STMAC, combining the merits of the PCF and DCF modes. In the PCF mode, the vehicles register their mobility information in RSU for time slot reservation, and they then receive their channel access time slots from a beacon frame transmitted by an RSU. In the DCF mode, the vehicles concurrently transmit their safety messages to their neighboring vehicles through the spatio-temporal coordination. We theoretically analyzed the performance of STMAC, and conducted extensive simulations to verify the analysis. The results show that STMAC outperforms the legacy MAC protocols using either PCF or DCF mode even in a highly congested road traffic condition. Thus, through STMAC, a new perspective for designing a MAC protocol for driving safety in vehicular environments is demonstrated.

For future work, we will extend our STMAC to support data services (e.g., multimedia streaming and interactive video call) for high data throughput rather than for short packet delivery time. Also, we will study a traffic-light-free communication protocol for autonomous vehicles passing intersection without the coordination of a traffic light. For a highway scenario, we will study an efficient communication protocol for driving safety.

APPENDIX A
CONTENTION PERIOD ADAPTATION

For a particular number of vehicles N , we can find an optimal p that can give the best successful probability g_N for each vehicle to send a registration request, so through

$$\frac{dg_N}{dp} = N \cdot (1-p)^{N-1} - N \cdot (N-1) \cdot p \cdot (1-p)^{N-2} = 0, \quad (13)$$

we can obtain an optimal p :

$$p = \frac{1}{N}. \quad (14)$$

Accordingly, the optimal g_N is:

$$g_N = \left(1 - \frac{1}{N}\right)^{N-1}. \quad (15)$$

The average number of slots to register one vehicle among N vehicles based on Equation (4) is:

$$M_N = \frac{1}{g_N} = \frac{1}{N \cdot p \cdot (1-p)^{N-1}}. \quad (16)$$

After a vehicle is registered with M_N , M_{N-1} for only $N-1$ vehicles is computed in the same way:

$$M_{N-1} = \frac{1}{g_{N-1}} = \frac{1}{(N-1) \cdot p \cdot (1-p)^{N-2}}. \quad (17)$$

Therefore, the total number of slot to register N vehicles is:

$$M = \sum_{i=N}^1 \frac{1}{g_i} = \sum_{i=N}^1 \frac{1}{i \cdot p \cdot (1-p)^{i-1}}. \quad (18)$$

APPENDIX B
MAXIMUM COMPATIBLE SET ALGORITHM

To construct a set-cover, the STMAC-Set-Cover algorithm in Algorithm 1 searches for a maximum compatible cover-set, using *Search_Max-Compatible-Cover-Set*(G, E') with the LoC graph G and the edge set E' in Algorithm 2. The remaining edges of this edge set E' are used for further compatible cover-sets for concurrent communications in G .

Algorithm 2 Search-Max-Compatible-Cover-Set Algorithm

```

1: function SEARCH_MAX_COMPATIBLE_COVER_SET
   ( $G, E'$ ) ▷  $G$  is the LoC graph and  $E'$  is the set of the
   remaining edges not belonging to any cover-set
2:  $V' \leftarrow \emptyset$  ▷  $V' (\subseteq V)$  is for a set of vertices with
   directed edges in  $E'$  and initialized with  $\emptyset$ 
3:  $M_{max} \leftarrow \emptyset$  ▷  $M_{max}$  is for a maximum compatible
   cover-set and initialized with zero
4: for all edges  $e_{i,j} \in E'$  do
5:    $V' \leftarrow V' \cup \{v_i, v_j\}$ 
6: end for
7: for each vertex  $s \in V'$  do
8:    $M \leftarrow \text{Make\_Maximal\_Compatible\_}$ 
    $\text{Set}(G, V', E', s)$ 
9:   if  $|M_{max}| < |M|$  then
10:     $M_{max} \leftarrow M$ 
11:   end if
12: end for
13: return  $M_{max}$ 
14: end function

```

Algorithm 2 searches for a maximum compatible cover-set among maximal compatible cover-sets constructed by *Make_Maximal-Compatible-Set*(G, V', E', s) in Algorithm 3. Algorithm 2 takes as input E' that is a set of edges not belonging to any compatible cover-set and it returns the maximum compatible cover-set, M_{max} . V' is for a set of vertices with directed edges in E' . Lines 2-3 initialize the V' and M_{max} to \emptyset . In lines 4-6, V' is a set of vertices such that v_i and v_j are linked with any directed edges $e_{i,j}$ in E' . For each vertex s in V' as a start node (i.e., root vertex) for breadth-first search (BFS) [21], we find a candidate maximal compatible set, M . In lines 7-12, if the number of elements in M is bigger than that of M_{max} , M is set to M_{max} . After running the for-loop in lines 7-12, consequently, M_{max} is returned as a maximum compatible cover set for the given edge set E' .

Algorithm 3 computes a maximal compatible cover set with s as a starting vertex for BFS along with interference range. The input parameters in Algorithm 3 are G as the LoC graph, V' as the set of vertices for the remaining edges in E' , E' as the remaining edge set, and s as a start node for BFS in the subgraph corresponding to $G(V', E')$.

Algorithm 3 Make-Maximal-Compatible-Set Algorithm

```

1: function MAKE_MAXIMAL_COMPATIBLE_SET
   ( $G, V', E', s$ ) ▷  $G$  is the LoC graph,  $V'$  is the set of
   vertices with directed edges in  $E'$ ,  $E'$  is the remaining
   edge set, and  $s$  is a start node for breadth-first search
2:  $G' \leftarrow \text{Graph}(V', E')$ 
3:  $G'' \leftarrow \text{Undirected\_Graph}(G')$ 
4:  $E_{max} \leftarrow \emptyset$ 
5:  $T \leftarrow \emptyset$ 
6:  $I \leftarrow \emptyset$ 
7: for each vertex  $u \in V' - \{s\}$  do
8:    $u.color \leftarrow \text{WHITE}$ 
9:    $u.degree \leftarrow 0$ 
10:   $u.receivers \leftarrow \emptyset$ 
11: end for
12:  $s.color \leftarrow \text{GRAY}$ 
13:  $s.degree \leftarrow 0$ 
14:  $Q \leftarrow \emptyset$ 
15:  $\text{Enqueue}(Q, s)$ 
16: while  $Q \neq \emptyset$  do
17:    $u \leftarrow \text{Dequeue}(Q)$ 
18:    $count \leftarrow 0$ 
19:    $I \leftarrow \text{Interference\_Set}(G, T)$ 
20:   for each vertex  $v \in N_{G''}(u)$  do
21:     if ( $v.color = \text{WHITE}$ ) or ( $v.color = \text{GRAY}$ 
       and  $v.degree = 0$ ) then
22:       if  $v \in N_{G'}(u)$  and  $u.degree = 0$  and  $v \notin I$ 
         then
23:          $E_{max} \leftarrow E_{max} \cup \{e_{uv}\}$ 
24:          $v.degree \leftarrow 1$ 
25:          $count \leftarrow count + 1$ 
26:          $u.receivers \leftarrow u.receivers \cup \{v\}$ 
27:       end if
28:        $v.color \leftarrow \text{GRAY}$ 
29:        $\text{Enqueue}(Q, v)$ 
30:     end if
31:   end for
32:   if  $count > 0$  then
33:      $u.degree \leftarrow count$ 
34:      $u.color \leftarrow \text{BLACK}$ 
35:      $T \leftarrow T \cup \{u\}$ 
36:   end if
37: end while
38: return  $E_{max}$ 
39: end function

```

Lines 5-6 make a transmission set and an interference set for a tripartite graph about the relationship between transmitters and interfered vehicles via each transmitter's receivers. In line 5, a transmission set T will contain transmitters in the compatible cover-set in the LoC subgraph G' for the current time slot. In line 6, an interference set I will contain vehicles which get the interference from a transmitter $t \in T$ in the LoC graph G . In lines 7-11, the color and degree of each vertex $u \in V' - \{s\}$ are set to *WHITE* as an unvisited vertex and 0, respectively. Also, the set of u 's receivers (*i.e.*, $u.receivers$)

is set to \emptyset . In lines 12-13, the color and degree of the start node s are set to *GRAY* and 0, respectively. In lines 14-15, a first-in-first-out (FIFO) queue Q is constructed, and the start node s is enqueued for BFS. In lines 16-37, edges $e_{uv} \in E'$ are added to the maximal compatible cover-set E_{max} . In lines 17-18, u is the front vertex dequeued from Q and $count$ for u 's outgoing degree is initialized with 0. Remarkably, in line 19, an interference set I is computed by $\text{Interference_Set}(G, T)$ along with the current transmission set T in the compatible cover-set for a time slot on the LoC graph G . For each transmitter $t \in T$, $\text{Interference_Set}(G, T)$ searches for white, interfered vertices $i \in I$ that are adjacent to t 's receiver in the LoC G . In lines 20-31, for each vertex v that is an adjacent vertex to u in the undirected LoC subgraph G'' , it is determined to add the edge e_{uv} to E_{max} by checking whether or not the receiver v is under the interference of any vertex $i \in I$. In lines 21-30, if v is a white vertex (*i.e.*, unvisited vertex) or a gray vertex with its degree 0 (*i.e.*, visited vertex, but neither transmitter nor receiver), and also if v is an adjacent vertex to u in the directed LoC subgraph G' , u has not yet been selected as a transmitter, and v is not under the interference of any other vertex $i \in I$, then the edge e_{uv} is added to E_{max} , v 's incoming degree is set to 1, u 's outgoing degree increases by 1 with $count$, v is added to the u 's receiver set $u.receivers$, and v is enqueued into Q for the further expansion of the BFS tree. Otherwise, if v is only a white vertex and the condition in line 22 is false, then v is enqueued into Q for the further expansion of the BFS tree. In lines 32-36, if the $count$ is positive, then u 's outgoing degree is set to $count$, and u is added to the transmission set T as a black vertex. Finally, after finishing the while-loop in lines 16-37, a maximal compatible cover-set E_{max} is returned.

REFERENCES

- [1] J. Harding *et al.*, "Vehicle-to-vehicle communications: readiness of V2V technology for application," Nat. Highway Traffic Safety Admin., Washington, DC, USA, Tech. Rep. DOT HS 812 014, 2014.
- [2] Y. L. Morgan, "Notes on DSRC & WAVE standards suite: Its architecture, design, and characteristics," *IEEE Commun. Surveys Tuts.*, vol. 12, no. 4, pp. 504–518, 4th Quart., 2010.
- [3] ASTM International, "Standard specification for telecommunications and information exchange between roadside and vehicle systems – 5 GHz band dedicated short range communications (DSRC) medium access control (MAC) and physical layer (PHY) specifications," ASTM, West Conshohocken, PA, USA, Tech. Rep. ASTM E2213-03(2010), 2010, pp. 1–25.
- [4] *IEEE Standard for Information Technology–Telecommunications and Information Exchange Between Systems Local and Metropolitan Area Networks–Specific Requirements Part 11: Wireless LAN Medium Access Control (MAC) and Physical Layer (PHY) Specifications*, IEEE Standard 802.11-2012 and IEEE Standard 802.11-2007), Mar. 2012, pp. 1295–1303.
- [5] *IEEE Guide for Wireless Access in Vehicular Environments (WAVE)–Architecture*, IEEE Standard 1609.0-2013, Mar. 2014, pp. 1–78.
- [6] S. Eichler, "Performance evaluation of the IEEE 802.11 p WAVE communication standard," in *Proc. IEEE 66th Veh. Technol. Conf.*, Sep. 2007, pp. 2199–2203.
- [7] Z. Wang and M. Hassan, "How much of DSRC is available for non-safety use?" in *Proc. 5th ACM Int. Workshop Veh. Inter-Networking (VANET)*, New York, NY, USA, 2008, pp. 23–29.
- [8] S. Subramanian, M. Werner, S. Liu, J. Jose, R. Lupoiae, and X. Wu, "Congestion control for vehicular safety: Synchronous and asynchronous MAC algorithms," in *Proc. 9th ACM Int. Workshop Veh. Inter-Networking, Syst., Appl. (VANET)*, New York, NY, USA, 2012, pp. 63–72.

- [9] T. V. Nguyen, F. Baccelli, K. Zhu, S. Subramanian, and X. Wu, "A performance analysis of CSMA based broadcast protocol in VANETs," in *Proc. IEEE INFOCOM*, Apr. 2013, pp. 2805–2813.
- [10] K.-T. Feng, "LMA: Location- and mobility-aware medium-access control protocols for vehicular ad hoc networks using directional antennas," *IEEE Trans. Veh. Technol.*, vol. 56, no. 6, pp. 3324–3336, Nov. 2007.
- [11] J.-M. Chung, M. Kim, Y.-S. Park, M. Choi, S. Lee, and H. S. Oh, "Time coordinated V2I communications and handover for WAVE networks," *IEEE J. Sel. Areas Commun.*, vol. 29, no. 3, pp. 545–558, Mar. 2011.
- [12] Y.-B. Ko, V. Shankarkumar, and N. H. Vaidya, "Medium access control protocols using directional antennas in ad hoc networks," in *Proc. IEEE INFOCOM*, vol. 1. Mar. 2000, pp. 13–21.
- [13] Q. Wang, S. Leng, H. Fu, and Y. Zhang, "An IEEE 802.11p-based multichannel MAC scheme with channel coordination for vehicular ad hoc networks," *IEEE Trans. Intell. Transp. Syst.*, vol. 13, no. 2, pp. 449–458, Jun. 2012.
- [14] K. A. Hafeez, L. Zhao, J. W. Mark, X. Shen, and Z. Niu, "Distributed multichannel and mobility-aware cluster-based MAC protocol for vehicular ad hoc networks," *IEEE Trans. Veh. Technol.*, vol. 62, no. 8, pp. 3886–3902, Oct. 2013.
- [15] D. N. M. Dang, C. S. Hong, S. Lee, and E.-N. Huh, "An efficient and reliable MAC in VANETs," *IEEE Commun. Lett.*, vol. 18, no. 4, pp. 616–619, Apr. 2014.
- [16] V. Nguyen, T. Z. Oo, P. Chuan, and C. S. Hong, "An efficient time slot acquisition on the hybrid TDMA/CSMA multichannel MAC in VANETs," *IEEE Commun. Lett.*, vol. 20, no. 5, pp. 970–973, May 2016.
- [17] J. Lee and C. M. Kim, "A roadside unit placement scheme for vehicular telematics networks," in *Proc. LNCS*, vol. 6059. 2010, pp. 196–202.
- [18] P. G. Lopez *et al.*, "Edge-centric computing: Vision and challenges," *SIGCOMM Comput. Commun. Rev.*, vol. 45, no. 5, pp. 37–42, Sep. 2015.
- [19] Garmin Ltd. *Garmin Automotive*, accessed on 2017. [Online]. Available: <https://www.garmin.com/en-US/>
- [20] Waze. *Waze Smartphone App for Navigator*, accessed on 2017. [Online]. Available: <https://www.waze.com>
- [21] T. H. Cormen, C. E. Leiserson, R. L. Rivest, and C. Stein, *Introduction to Algorithms*, 3rd ed. Cambridge, MA, USA: MIT Press, 2009.
- [22] K. Kim, J. Lee, and W. Lee, "A MAC protocol using road traffic estimation for infrastructure-to-vehicle communications on highways," *IEEE Trans. Intell. Transp. Syst.*, vol. 14, no. 3, pp. 1500–1509, Sep. 2013.
- [23] M. S. Sharawi, F. Sultan, and D. N. Aloii, "An 8-element printed V-shaped circular antenna array for power-based vehicular localization," *IEEE Antennas Wireless Propag. Lett.*, vol. 11, pp. 1133–1136, 2012.
- [24] D. Gesbert, M. Kountouris, R. W. Heath, Jr., C.-B. Chae, and T. Sälzer, "Shifting the MIMO paradigm," *IEEE Signal Process. Mag.*, vol. 24, no. 5, pp. 36–46, Sep. 2007.
- [25] N. Razavi-Ghods, M. Abdalla, and S. Salous, "Characterisation of MIMO propagation channels using directional antenna arrays," in *Proc. 5th IEEE Int. Conf. 3G Mobile Commun. Technol.*, Oct. 2004, pp. 163–167.
- [26] V. Kawadia and P. R. Kumar, "Principles and protocols for power control in wireless ad hoc networks," *IEEE J. Sel. Areas Commun.*, vol. 23, no. 1, pp. 76–88, Jan. 2005.
- [27] F. Schmidt-Eisenlohr, M. Torrent-Moreno, T. Mittag, and H. Hartenstein, "Simulation platform for inter-vehicle communications and analysis of periodic information exchange," in *Proc. 4th Annu. Conf. Wireless Demand Netw. Syst. Ser.*, Jan. 2007, pp. 50–58.
- [28] New York State Department of Motor Vehicles. *Driver's Manual*, accessed on 2017. [Online]. Available: <https://dmv.ny.gov/>
- [29] K. Xu, M. Gerla, and S. Bae, "How effective is the IEEE 802.11 RTS/CTS handshake in ad hoc networks," in *Proc. IEEE Global Telecommun. Conf. (GLOBECOM)*, vol. 1. Nov. 2002, pp. 72–76.
- [30] L. G. Roberts, "ALOHA packet system with and without slots and capture," *ACM SIGCOMM Comput. Commun. Rev.*, vol. 5, no. 2, pp. 28–42, 1975.
- [31] W. Crowther, R. Rettberg, D. Waldem, S. Ornstein, and F. Heart, "A system for broadcast communication: Reservation-ALOHA," in *Proc. 6th Hawaii Internat. Conf. Syst. Sci.*, Jan. 1973, pp. 596–603.
- [32] R. K. Lam and P. R. Kumar, "Dynamic channel reservation to enhance channel access by exploiting structure of vehicular networks," in *Proc. IEEE 71st Veh. Technol. Conf. (VTC-Spring)*, May 2010, pp. 1–5.
- [33] *IEEE Standard for Wireless Access in Vehicular Environments (WAVE)—Multi-Channel Operation, 1609 WG—Dedicated Short Range Communication Working Group*, IEEE Standard 1609.4-2016 and IEEE Standard 1609.4-2010, Mar. 2016, pp. 1–94.
- [34] G. Bianchi, "Performance analysis of the IEEE 802.11 distributed coordination function," *IEEE J. Sel. Areas Commun.*, vol. 18, no. 3, pp. 535–547, Mar. 2000.
- [35] J. Hui and M. Devetsikiotis, "A unified model for the performance analysis of IEEE 802.11e EDCA," *IEEE Trans. Commun.*, vol. 53, no. 9, pp. 1498–1510, Sep. 2005.
- [36] Z.-N. Kong, D. H. K. Tsang, B. Bensaou, and D. Gao, "Performance analysis of IEEE 802.11e contention-based channel access," *IEEE J. Sel. Areas Commun.*, vol. 22, no. 10, pp. 2095–2106, Dec. 2004.
- [37] Y. Yao, L. Rao, X. Liu, and X. Zhou, "Delay analysis and study of IEEE 802.11 p based DSRC safety communication in a highway environment," in *Proc. IEEE INFOCOM*, Apr. 2013, pp. 1591–1599.
- [38] OpenStreetMap. *Open Street Map for Road Maps*, accessed on 2017. [Online]. Available: <http://www.openstreetmap.org>
- [39] OMNeT++. *Network Simulation Framework*, accessed on 2017. [Online]. Available: <http://www.omnetpp.org>
- [40] C. Sommer, R. German, and F. Dressler, "Bidirectionally coupled network and road traffic simulation for improved IVC analysis," *IEEE Trans. Mobile Comput.*, vol. 10, no. 1, pp. 3–15, Jan. 2011.
- [41] D. Krajzewicz, J. Erdmann, M. Behrisch, and L. Bieker, "Recent development and applications of SUMO—Simulation of urban MOBility," *Int. J. Adv. Syst. Meas.*, vol. 5, nos. 3–4, pp. 128–138, Dec. 2012.
- [42] T. K. Mak, K. P. Laberteaux, and R. Sengupta, "A multi-channel VANET providing concurrent safety and commercial services," in *Proc. 2nd ACM Int. Workshop Veh. Ad Hoc Netw. (VANET)*, New York, NY, USA, 2005, pp. 1–9.



Jaehoon (Paul) Jeong received the B.S. degree from the Department of Information Engineering, Sungkyunkwan University, in 1999, the M.S. degree from the School of Computer Science and Engineering, Seoul National University, South Korea, in 2001, and the Ph.D. degree from the Department of Computer Science and Engineering, University of Minnesota, in 2009. He is currently an Assistant Professor with the Department of Software, Sungkyunkwan University. His research interests include Internet of Things, vehicular networks, wireless sensor networks, and mobile ad hoc networks. He is a member of the ACM and the IEEE Computer Society.



Yiwen (Chris) Shen received the B.S. degree from the Department of Communication Engineering, North University of China, in 2009, and the M.S. degree from the Department of Mechatronics Engineering, North University of China, in 2013. He is currently pursuing the Ph.D. degree with the Department of Computer Science & Engineering, Sungkyunkwan University, South Korea. His research interests include intelligent transportation systems, vehicular ad hoc networks, and wireless communications. He received the China State Scholarship from the China Scholarship Council.



Sangsoo Jeong received the B.S. degree from the Department of Computer Software, Gachon University, Seongnam, South Korea, in 2013. He is currently pursuing the Ph.D. degree with the Department of Information and Communication Engineering, DGIST. His research areas include cyber-physical systems, smart city, vehicular ad-hoc networks (VANETs), and Internet of Things (IoT).



Sejun Lee received the B.S. degree from the School of Information and Communication Engineering, Mokpo National Maritime University, South Korea, in 2014, and the M.S. degree from the Department of Computer Science and Engineering, Sungkyunkwan University, South Korea, under the supervision of J. Jeong. He is currently a Researcher with the Korea Electronics Technology Institute. His research areas include vehicular ad-hoc networks, cyber-physical systems, and internet of things.

1294
1295
1296
1297
1298
1299
1300
1301
1302
1303
1304
1305



Hwanseok (Harrison) Jeong (S'14) received the B.S. degree from the Department of Computer Engineering, Kyungpook National University, in 1999, and the M.S. degree from the School of Computer Science and Engineering, Seoul National University, in 2001. He is currently pursuing the Ph.D. degree with the Department of Computer Engineering, Sungkyunkwan University. He has been with SK Telecom as a Research and Development Strategist, and the Technical Engineer in Seoul, South Korea, since 2001. His research interests include vehicular ad-hoc networks, mobile ad hoc networks, and cyber-physical systems.

1306
1307
1308
1309
1310
1311
1312
1313
1314
1315
1316
1317
1318



Tae (Tom) Oh (SM'09) received the B.S. degree in electrical engineering from Texas Tech University in 1991, and the M.S. and Ph.D. degrees in electrical engineering from Southern Methodist University in 1995 and 2001, respectively, while working for telecommunication and defense companies. He is currently an Associate Professor with the Department of Information Sciences and Technologies and the Department of Computing Security, Rochester Institute of Technology. His research includes mobile ad hoc networks, vehicle area networks, sensor networks, and mobile device security. He is a member of the ACM.

1319
1320
1321
1322
1323
1324
1325
1326
1327
1328
1329
1330
1331



Taejoon Park (M'05) received the B.S. degree in electrical engineering from Hongik University, Seoul, South Korea, in 1992, the M.S. degree in electrical engineering from the Korea Advanced Institute of Science and Technology Daejeon, South Korea, in 1994, and the Ph.D. degree in electrical engineering and computer science from the University of Michigan, Ann Arbor, MI, USA, in 2005. He is currently a Professor with the Department of Robotics Engineering, Hanyang University, South Korea. His current research interests include in cyber-physical systems, Internet of Things, and their applications to robots and vehicles. He is a member of the ACM.



Muhammad Usman Ilyas received the B.E. degree (Hons.) in electrical engineering from the National University of Sciences and Technology (NUST), Islamabad, Pakistan, in 1999, the M.S. degree in computer engineering from the Lahore University of Management Sciences, Lahore, Pakistan, in 2004, and the M.S. and Ph.D. degrees in electrical engineering from Michigan State University in 2007 and 2009, respectively. He is currently appointed as an Assistant Professor of Electrical Engineering with the School of Electrical Engineering and Computer Science, NUST. He is also an Assistant Professor in the Department of Computer Science in the Faculty of Computing and Information Technology, University of Jeddah in Saudi Arabia.

1332
1333
1334
1335
1336
1337
1338
1339
1340
1341
1342
1343
1344
1345



Sang Hyuk Son (F'13) received the B.S. degree in electronics engineering from Seoul National University, the M.S. degree from KAIST, and the Ph.D. degree in computer science from the University of Maryland at College Park, College Park. He is currently the President of DGIST. He has been a Professor with the Computer Science Department, University of Virginia, and the WCU Chair Professor with Sogang University. His research interests include cyber physical systems, real-time and embedded systems, database and data services, and wireless sensor networks.

1346
1347
1348
1349
1350
1351
1352
1353
1354
1355
1356
1357



David H. C. Du (F'98) received the B.S. degree in mathematics from National Tsing-Hua University, Taiwan, in 1974, and the M.S. and Ph.D. degrees in computer science from the University of Washington, Seattle, in 1980 and 1981, respectively. He is currently the Qwest Chair Professor with the Computer Science and Engineering Department, University of Minnesota, Minneapolis. His research interests include cyber security, sensor networks, multimedia computing, storage systems, and high-speed networking.

1358
1359
1360
1361
1362
1363
1364
1365
1366
1367
1368

STMAC: Spatio-Temporal Coordination-Based MAC Protocol for Driving Safety in Urban Vehicular Networks

Jaehoon Jeong, *Member, IEEE*, Yiwen Shen, *Student Member, IEEE*, Sangsoo Jeong, *Student Member, IEEE*, Sejun Lee, *Student Member, IEEE*, Hwanseok Jeong, *Student Member, IEEE*, Tae Oh, *Senior Member, IEEE*, Taejoon Park, *Member, IEEE*, Muhammad Usman Ilyas, *Member, IEEE*, Sang Hyuk Son, *Fellow, IEEE*, and David H. C. Du, *Fellow, IEEE*

Abstract—In this paper, we propose a spatio-temporal coordination-based media access control (STMAC) protocol for efficiently sharing driving safety information in urban vehicular networks. STMAC exploits a unique spatio-temporal feature characterized from a geometric relation among vehicles to form a line-of-collision graph, which shows the relationship among vehicles that may collide with each other. Based on this graph, we propose a contention-free channel access scheme to exchange safety messages simultaneously by employing directional antenna and transmission power control. Based on an urban road layout, we propose an optimized contention period schedule by considering the arrival rate of vehicles at an intersection in the communication range of a road-side unit to reduce vehicle registration time. Using theoretical analysis and extensive simulations, STMAC outperformed legacy MAC protocols especially in a traffic congestion scenario. In the congestion case, STMAC can reduce the average superframe duration by 66.7%, packet end-to-

end delay by 68.3%, and packet loss ratio by 88% in comparison with the existing MAC protocol based on the IEEE 802.11p.

Index Terms—Vehicular networks, spatio-temporal, safety, MAC protocol, coordination.

I. INTRODUCTION

DRIVING safety is one of the most important issues since approximately 1.24 million people die each year globally as a result of traffic accidents. Vehicular ad hoc networks (VANETs) have been highlighted and implemented during the last decade to support wireless communications for driving safety in road networks [1], [2]. Driving safety can be improved by an assistance of rapid exchanged of driving information among neighboring vehicles. As an important trend, dedicated short-range communications (DSRC) [3] were standardized as IEEE 802.11p in 2010 (now incorporated into IEEE 802.11 protocols [4]) for wireless access in vehicular environments (WAVE) [2], [5]. IEEE WAVE protocol is a multichannel MAC protocol [4], adopting the enhanced distributed channel access (EDCA) [5] for quality of service (QoS) in vehicular environments. Many research results [6]–[9] published that a performance of WAVE deteriorates when a density of vehicles is high, approaching the performance of a slotted ALOHA process [8]. As a result, many other MAC protocols [10]–[16] have been proposed to improve the performance of WAVE. However, the MAC protocols were not designed to support the geometric relation among vehicles for the driving safety and didn't consider the configuration of urban roads.

A MAC protocol can operate in a distributed coordination function (DCF) mode (i.e., contention based), a point coordination function (PCF) mode (i.e., contention-free based) or a hybrid coordination function (HCF) mode [4]. For driving safety in vehicular environments, a MAC protocol in the DCF-mode executes based on carrier sense multiple access with collision avoidance (CSMA/CA) [4] mechanism. This distributed approach can incur high frame collision rates at congested intersections in an urban area [6]–[9], and in the case of a lack of comprehensive vehicle traffic. As a result, it may lead to an unreliable, non-prompt data exchange. On the contrary, a MAC protocol in the PCF-mode can wield roadside units (RSUs) or access points (APs) as coordinators to

Manuscript received September 19, 2016; revised March 4, 2017 and May 24, 2017; accepted July 2, 2017. This work was supported in part by the Basic Science Research Program through the National Research Foundation of Korea (NRF) funded by the Ministry of Science, ICT & Future Planning (MSIP) under Grant 2014R1A1A1006438, in part by the Ministry of Education under Grant 2017R1D1A1B03035885, and in part by the Global Research Laboratory Program through the NRF and the DGIST Research and Development Program (CPS Global Center) funded by the MSIP under Grant 2013K1A1A2A02078326. The Associate Editor for this paper was L. Li. (Corresponding author: Sang Hyuk Son.)

J. Jeong is with the Department of Interaction Science, Sungkyunkwan University, Suwon 16419, South Korea (e-mail: pauljeong@skku.edu).

Y. Shen and H. Jeong are with the Department of Computer Science & Engineering, Sungkyunkwan University, Suwon 16419, South Korea (e-mail: chrishshen@skku.edu; harryjeong@skku.edu).

S. Lee is with the Korea Electronics Technology Institute, Seongnam-si 13509, South Korea (e-mail: sejunlee@skku.edu).

S. Jeong and S. H. Son are with the Department of Information and Communication Engineering, DGIST, Daegu 42988, South Korea (e-mail: 88jeongss@dgist.ac.kr; son@dgist.ac.kr).

T. Oh is with the Department of Information Sciences & Technologies, Rochester Institute of Technology, Rochester, NY 14623-5603 USA (e-mail: tom.oh@rit.edu).

T. Park is with the Department of Robotics Engineering, Hanyang University, Seoul 04763, South Korea (e-mail: taejoon@hanyang.ac.kr).

M. U. Ilyas is with the Department of Electrical Engineering, National University of Sciences and Technology, Islamabad 44000, Pakistan, and also with the Department of Computer Science, Faculty of Computing and Information Technology, University of Jeddah, Jeddah 21589, Saudi Arabia (e-mail: usman.ilyas@seecs.edu.pk; milyas@uj.edu.sa).

D. H. C. Du is with the Department of Computer Science & Engineering, University of Minnesota, Minneapolis, MN 55455 USA (e-mail: du@cs.umn.edu).

Color versions of one or more of the figures in this paper are available online at <http://ieeexplore.ieee.org>.

Digital Object Identifier 10.1109/TITS.2017.2723946

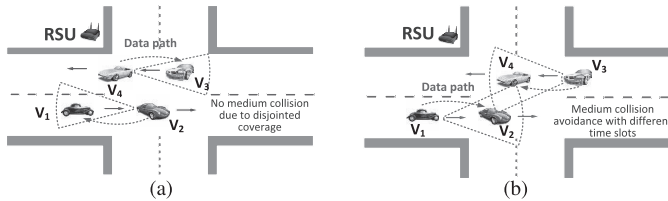


Fig. 1. Spatial and temporal coordination. (a) Spatial coordination. (b) Temporal coordination.

a temporal feature by which the communications should be separated for collision avoidance. Further, based on the urban road layout, we propose a scheme that optimizes the contention period for vehicle registration into an RSU by reducing the contention duration by considering the vehicle arrival rate at an intersection. Our STMAC can facilitate the rapid exchange of driving information among neighboring vehicles. This rapid exchange can help drivers to get driving assistance information for avoiding possible collisions. Even in self-driving, STMAC can help autonomous vehicles avoid collision by exchanging the mobility information and cooperating with each other for driving coordination.

The contributions of this paper are as follows:

- **An LoC graph based channel access scheme via an enhanced set-cover algorithm is proposed:** STMAC's set-cover algorithm handles an *unfixed* subsets family of elements where each subset is covered by a time slot, and each element is a transmission, which differs from the legacy set-cover algorithm [21] handling a *fixed* subset family of elements. This algorithm schedules multiple vehicles to transmit their safety messages simultaneously in spatially disjointed transmission areas (see Section IV-A).
- **A contention period optimization is proposed for the efficient channel usage:** STMAC's contention period adapts the vehicle arrival rate at an intersection in an urban area for better channel utilization. This optimization is feasible in vehicular networks where vehicles move along confined roadways (see Section IV-B).
- **A new hybrid MAC protocol is proposed using spatio-temporal coordination:** STMAC uses the PCF mode to register vehicles for a time slot allocation as well as an emergency message dissemination from an RSU to vehicles. It uses the DCF mode for both safety message exchange and emergency message dissemination among vehicles by *spatio-temporal coordination*. (see Section V).

Through theoretical analysis and extensive simulations, it is shown that STMAC outperforms other state-of-the-art protocols in terms of average superframe duration, end-to-end (E2E) delay, and packet loss ratio.

The remainder of this paper is organized as follows. In Section II, related work is summarized along with analysis. Section III discusses the assumptions and scenarios used for problem formulation. Section IV describes the characterization of spatial-temporal features and the optimization of the contention period. In Section V, the STMAC protocol is proposed. In Section VI, we evaluate STMAC by comparing with baseline MAC protocols (*i.e.*, PCF and DCF MAC protocols) through theoretical data and simulation results. Finally, Section VII concludes this paper along with future work.

II. RELATED WORK

IEEE 802.11 [4] defines an HCF-mode to use a contention-based channel access method for contention-based transfer, called the enhanced distributed channel access (EDCA), and a controlled channel access for contention-free transfer, called

59 schedule time slots for transmitters. This centralized approach
 60 can reduce frame collision rates and guarantees a certain
 61 delay bound, but increases a data delivery delay since multiple
 62 transmitters must be managed. The HCF mode, which is a part
 63 of IEEE 802.11 [4], combines the PCF and DCF modes with
 64 QoS enhancement feature to deliver QoS data from vehicles
 65 to an RSU (*i.e.*, AP). The HCF mode employs the HCF
 66 controlled channel access (HCCA) [4] as the PCF-mode for
 67 contention-free transfer, and the EDCA [4] mechanism as the
 68 DCF-mode for contention-based transfer. However, tailoring
 69 optimal combination of the PCF and DCF modes still remains
 70 challenging research issues for the driving safety in vehicular
 71 environment.

72 On the other hand, for efficient communication among
 73 vehicles, RSUs are expected to be deployed at intersections
 74 and streets in vehicular networks [17]. RSUs with powerful
 75 computation capabilities can operate as edge devices [18] to
 76 coordinate channel access for vehicles while preventing channel
 77 collision and provides Internet connectivity to disseminate
 78 safety information. Thus, a cost for RSU implementation can
 79 be easily justified by the reduction of human injuries and
 80 deaths as well as property loss caused by road accidents. Also,
 81 the implementation of geographical positioning system (GPS)
 82 is another important trend in vehicular networks. Navigators
 83 (*i.e.*, a dedicated GPS navigator [19] and a smartphone
 84 navigation app [20]) are commonly used by drivers who are
 85 driving to destinations in unfamiliar areas. An RSU can collect
 86 GPS data of vehicles in its coverage so that the transmission
 87 schedule of vehicles can be optimized. Therefore, RSUs can
 88 be used as coordinators to orchestrate communications among
 89 vehicles. However, few studies have explored the important
 90 functions of RSUs for driving safety.

91 In this paper, we propose a Spatio-Temporal coordination
 92 based MAC (STMAC) protocol for urban scenarios, utilizing
 93 a spatio-temporal feature and a road layout feature in
 94 urban areas for better wireless channel access in vehicular
 95 networks. The objective of STMAC is to support reliable
 96 and fast data exchange among vehicles for driving safety via
 97 the coordination of vehicular infrastructure, such as RSUs.
 98 STMAC leverages a unique spatio-temporal feature to form
 99 a line-of-collision (LoC) graph in which multiple vehicles
 100 can transmit in the same time slot without channel inter-
 101 ferences or collisions by utilizing directional antennas and
 102 transmission power control. As shown in Fig. 1(a), the spatial
 103 disjoint of communication areas enabled by directional anten-
 104 nas provides the feature of spatial reuse, whereas the overlap
 105 of the communication areas shown in Fig. 1(b) indicates

the HCF controlled channel access (HCCA) [4]. In contention-free transfer, the HCCA mechanism [4] enables the stations to transmit their QoS data to the AP according to the schedule made by the AP without any contention. On the other hand, the stations attempt to transmit their prioritized QoS data to the AP with the EDCA mechanism [4]. In both modes, the station transmits its data to its neighboring station under its communication coverage via the AP. For the purpose of driving safety, direct data delivery is possible through vehicle-to-vehicle (V2V) communication without using the data relay of an RSU. Thus, we need to design a new hybrid mode for a reliable and fast data delivery among vehicles.

Many other MAC protocols have been proposed, using MAC coordination functions (*i.e.*, DCF and PCF) to improve the efficiency and reliability of wireless media access in mobile ad hoc networks (MANETs) and vehicular ad hoc networks (VANETs). In most cases, omni-directional antenna is considered for MAC protocols even though directional antenna has several benefits. Therefore, the literature review of MAC protocols is discussed according to the coordination functions along with antenna types.

Ko *et al.* [12] propose a directional antenna MAC protocol (D-MAC) in DCF. For concurrent communications and based on D-MAC, Feng *et al.* propose a location- and mobility-aware (LMA) MAC protocol [10]. Both D-MAC and LMA perform communications in DCF mode utilizing CSMA/CA and the exponential backoff mechanism for ad hoc networks. LMA [10] is designed to achieve efficient V2V communication without infrastructure nodes (*e.g.*, RSU). The aim of LMA is to achieve efficient directional transmission while resolving the deafness problem [10]. Vehicles in LMA use the predicted location and mobility information of the target vehicle, thereby performing directed transmissions using beamforming. As an enhanced D-MAC protocol, LMA exploits the advantages of a directional antenna, such as spatial reuse, by considering the moving direction of a vehicle, and uses a longer transmission range in transmitting request-to-send (RTS), clear-to-send (CTS), data frame (DATA), and acknowledgment (ACK) as directed transmissions. However, the frame collisions increases substantially when both D-MAC and LMA are used when the vehicle density is high. This may result in a serious packet delivery delay, which is not acceptable for driving safety.

In PCF, Chung *et al.* propose a WAVE PCF MAC protocol (WPCF) [11] to improve the channel utilization and user capacity in vehicle-to-infrastructure (V2I) or infrastructure-to-vehicle (I2V) communication. The main purpose of WPCF is the dynamic reduction of the PCF interframe space (PIFS), in order to increase the channel efficiency when multiple vehicles attempt to sequentially communicate with an RSU [17]. WPCF also suggests a handover mechanism by adopting a WAVE handover controller to minimize service disconnection time [11]. However, since WPCF neither optimizes the length of a contention period (CP) nor utilizes concurrent transmissions in a contention-free period (CFP), the utilization of the wireless channel still needs to be improved. Unlike WPCF, which is a kind of HCF, STMAC allows vehicles to exchange their driving information with their neighboring

vehicles without the relaying of an RSU. Note that since WPCF is an Infrastructure-to-Vehicle (I2V) MAC protocol, the Vehicle-to-Vehicle (V2V) data delivery requires the relay via an RSU. Because this exchange is performed concurrently for the disjoint sets of vehicles, the packet delivery delay of STMAC is shorter than that of WPCF. Kim *et al.* propose a MAC protocol using a road traffic estimation for I2V communication in a highway environment [22]. Their MAC protocol estimates the road traffic to precisely control the transmission probability of vehicles in order to maximize system throughput. The protocol also presents a mechanism to use a threshold to limit the number of transmitted packets for fairness among vehicles. Hafeez *et al.* propose a distributed multichannel and mobility-aware cluster-based MAC protocol, called DMMAC [14]. DMMAC utilizes the EDCA of IEEE 802.11p to differentiate the types of packets, enables vehicles to form clusters based on a weighted stabilization factor to exchange packets.

Through the evaluation of the existing MAC protocols, we found that LMA, WPCF, and DMMAC are representatives of DCF, PCF, and cluster-based MAC protocols in VANET, respectively. Hence, the three protocols are used as baselines for performance evaluation in this paper. Comparing with LMA, WPCF, and DMMAC, STMAC leverages a spatio-temporal feature to improve the efficiency of channel access and reduce the delivery delay of safety messages. STMAC also considers an urban layout to reduce the length of the contention period. Therefore, the results will show that STMAC can outperform the legacy MAC protocols, such as LMA, WPCF, and DMMAC.

III. PROBLEM FORMULATION

The goal of the STMAC protocol is to provide a reliable and fast message exchange among adjacent vehicles through the coordination of an RSU for safe driving. To achieve this goal, a directed transmission is used whenever possible to maximize the number of concurrent transmissions through spatio-temporal transmission scheduling. The following section, we specify several assumptions and a target scenario.

A. Assumptions

The following assumptions are made in the course of designing STMAC:

- Vehicles are equipped with a DSRC interface [2] and a directional antenna array with the phase shifting [10], [23], whereas RSUs are equipped with an omnidirectional antenna. The directional antenna array can generate multiple beams toward multiple receivers at the same time (*e.g.*, MU-MIMO) [24], [25]. The narrow beam problem can be avoided in our STMAC. The direction of the each beam and the communication coverage (*i.e.*, R and β , where R is the communication range defined as a distance where a successful data frame from a sender vehicle can be transmitted to a receiver vehicle with almost no bit error, and β is the communication beam angle that is constructed by the

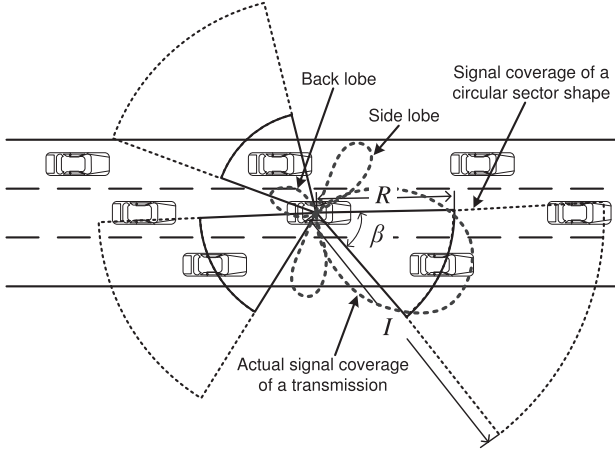


Fig. 2. A transmission signal coverage and interference range.

phase shifting of the directional antenna array [23]) are adjustable by locating the receiving vehicle's location and controlling RF transmission power [10], [23], [26], as shown in Fig. 2. The RF transmission power W_t can be determined as follows:

$$W_t = \frac{(2d)^\alpha \cdot (4\pi)^2 \cdot W_r}{\Lambda^2}, \quad (1)$$

where d is the distance between a transmitter and a receiver; α is the minimum path loss coefficient; Λ is the wavelength of a signal; W_r is the minimum power level to be able to physically receive a signal, which can be calculated by $W_r = 10^{sa/10}$, and sa is the minimum signal attenuation threshold.

- For simplicity, the interference range I of a transmission is considered to be two times the communication range R , as shown in Fig. 2, which is used in an algorithm (Algorithm 1 in Section IV-A) to decide an interference set when calculating a transmission schedule. Also, as shown in Fig. 2, a circular-sector-shape signal coverage is considered instead of the actual transmission signal coverage, and the side lobes and the back lobe are ignored for the simplicity of modeling.
- A procedure of handover similar to that of WPCF [11] is implemented in this work by using two DSRC service channels [2]. The first channel is used for the RSU's coverage, and the second channel is used for the adjacent RSU's coverage. The detailed description of the handover is given in WPCF [11].
- Vehicles are equipped with a GPS-based navigation system [19], [20]. This GPS navigation system provides vehicles with their position, speed, and direction at any time.
- The effect of buildings or trees (called terrain effect) exists in real vehicular networks. The Nakagami fading model [27] is usually used for vehicular networks. If a better fading model considering terrain effect is available, our STMAC protocol can accommodate such a model.

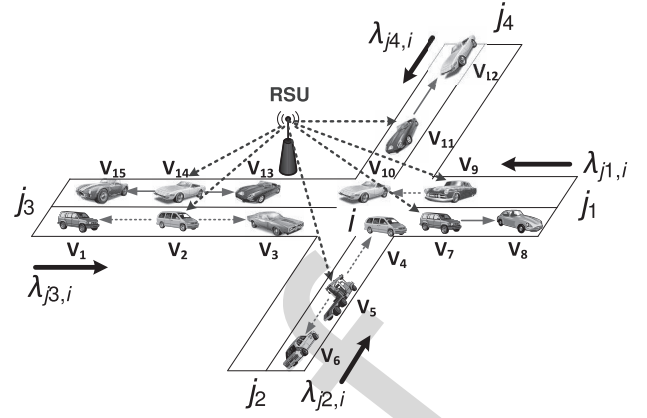


Fig. 3. The target scenario of spatio-temporal coordination by the RSU.

B. Target Scenario

Our target scenario is a vehicle data exchange, such as mobility information (e.g., location, direction, and speed) and in-vehicle device status (e.g., break, gear, engine, and axle), for driving safety in urban road networks. As shown in Fig. 3, RSUs are typically deployed at road intersections and serve as gateways between VANETs and the intelligent transportation systems (ITS) infrastructure [17]. An RSU's transmission coverage range is set to cover the maximum of the lengths of the halves of the road segments. The inter-RSU interference is avoided by letting two adjacent RSUs use different DSRC service channels. Vehicles periodically transmit time slot requests to an RSU along with their mobility information (i.e., current location, moving direction, and speed). The RSU uses the request information to construct a transmission schedule for the wireless channel access. Using the assigned time slots from the schedule, safety messages are directly exchanged between neighbor vehicles to prevent accidents. In the next section, we will explain the spatio-temporal feature and contention period optimization in STMAC protocol.

IV. SPATIO-TEMPORAL COORDINATION AND CONTENTION PERIOD OPTIMIZATION

In this section, we propose a new channel access scheme based on an enhanced set-cover algorithm by characterizing a spatio-temporal feature in urban vehicular networks. We also propose a contention period adaptation based on the vehicle arrival rate at an intersection in an urban area. To characterize the spatio-temporal feature in a vehicular environment, the formation of the line-of-collision (LoC) graph is first explained.

A. Spatio-Temporal Coordination Based Channel Access

In an urban area, a vehicle accident is usually a direct crash or collision among vehicles (e.g., frontal, side, and rear impacts). Preventing the initial direct crash can largely reduce fatalities and property losses. We propose an LoC graph among vehicles based on a geometric relation to describe the initial direct crash. As shown in Fig. 4, vehicles A and B have an LoC relation because there are no middle vehicles between them, and can therefore crash directly. From A, two tangent

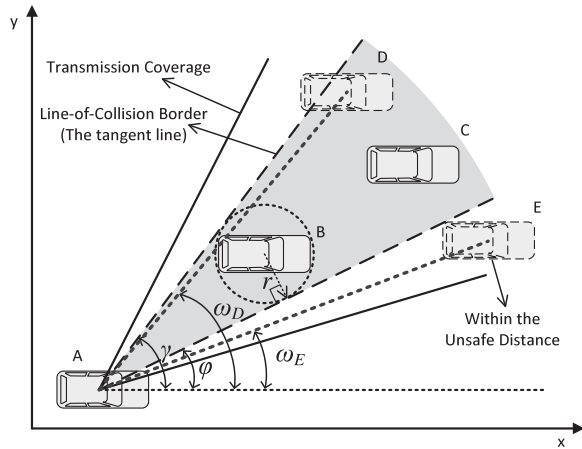


Fig. 4. Line-of-collision relation construction.

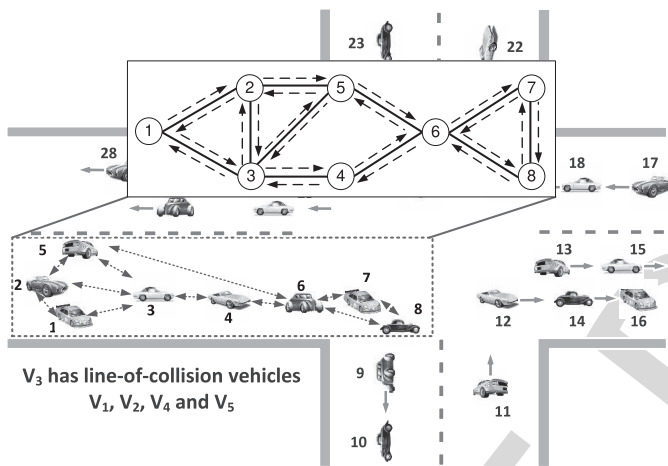
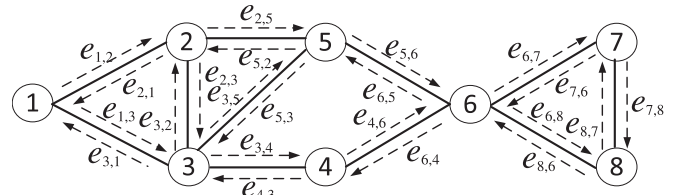


Fig. 5. Line-of-collision vehicles in road segment with multiple lanes.

349 lines on a circle can be derived based on the half length
 350 (as a radius r) of B . Any vehicle within the area between
 351 the two tangent lines (gray area in Fig. 4), but farther than
 352 B , is considered as a non-LoC vehicle to A , e.g., C in Fig. 4.
 353 By comparing the two angles γ and ϕ of the two tangent
 354 lines and the unsafe distance determined by the two-second
 355 rule [28], it can also be determined whether or not any other
 356 vehicles can be LoC vehicles of A . For example, D has no
 357 LoC relation with A because the angle ω_D is smaller than γ ,
 358 but larger than ϕ , and E is an LoC vehicle of A , based on
 359 the fact that the angle ω_E is smaller than ϕ and is within the
 360 unsafe distance. Note that vehicles with different sizes can
 361 be considered as the same class, e.g., a vehicle with a length
 362 smaller than 5 meters can be categorized as a 5 meter vehicle
 363 to determine the radius r . From communication collision point
 364 of view, if C is in the interference range of A , which is
 365 2 times transmission range of A , C can be interfered. But
 366 in our algorithm 1, this interference is avoided by scheduling
 367 vehicle A and C in different time slot, which means if C is
 368 in the interference range of A , when A is transmitting to B ,
 369 C will neither receiving nor sending a packet. Note that LoC
 370 means Line of Collision, which indicates the relationship of
 371 directly physically collision of two neighboring vehicles rather
 372 than the line-of-sight for communication range.



Start node	Edges in a time slot
3, 7	$S_1 = \{e_{3,1}, e_{3,2}, e_{3,4}, e_{3,5}, e_{7,6}, e_{7,8}\}$
2, 8	$S_2 = \{e_{2,1}, e_{2,3}, e_{2,5}, e_{8,6}, e_{8,7}\}$
1, 6	$S_3 = \{e_{1,2}, e_{1,3}, e_{6,4}, e_{6,5}, e_{6,7}, e_{6,8}\}$
5	$S_4 = \{e_{5,2}, e_{5,3}, e_{5,6}\}$
4	$S_5 = \{e_{4,3}, e_{4,6}\}$

Fig. 6. Searching sequence for maximum compatible cover-sets.

Based on the LoC relation, an LoC graph can be constructed. As shown in the dotted box of Fig. 5, we consider a scenario in which vehicles are moving in multiple lanes in road segments. The solid box in Fig. 5 shows an LoC graph $G = (V, E)$ constructed by the vehicles inside the dotted box, where the vertices in V are vehicles and the edges in E indicate an LoC relation between two adjacent vehicles that can collide directly with each other. Thus, the continuous communications are necessary for the connected vehicles in the LoC graph G . Notice that the LoC graph is used in our STMAC protocol to reduce medium collision, which is discussed in later in this section.

Through the LoC graph of the vehicles, we propose a spatio-temporal coordination based channel access scheme by using an enhanced set-cover algorithm. The enhanced set-cover algorithm for STMAC attempts to find a minimum set-cover for an optimal time slot allocation in a given LoC graph. Our STMAC Set-Cover algorithm attempts to allow as many concurrent transmissions as possible in each time slot in order to reduce the contention-free period for the required transmissions of all the LoC vehicles.

We define the following terms for the STMAC Set-Cover algorithm:

Definition 1 (Cover-Set): Let **Cover-Set** be a set S_i of edges in an LoC graph G where the edges are **mutually not interfering** (i.e., **compatible**) with each other, that is, any pair of edges $e_{u,v}, e_{x,y} \in E(G)$ are compatible with each other. For example, as shown in Fig. 6, the cover-set S_1 is $\{e_{3,1}, e_{3,2}, e_{3,4}, e_{3,5}, e_{7,6}, e_{7,8}\}$ for time slot 1.

Definition 2 (Set-Cover): Let **Set-Cover** be a set S of cover-sets S_i for $i = 1 \dots n$ that is equal to the edge set $E(G)$ such that $E(G) = \bigcup_{i=1}^n S_i$. That is, the set-cover S includes all the directed edges in an LoC graph G and represents the schedule of concurrent transmissions of the edges in S_i for time slot i . For example, Fig. 6 shows the mapping between time slot i and cover-set S_i .

We now formulate an optimization of a time slot allocation for cover-sets of non-interfering edges that can be transmitted concurrently. Let 2^N be a power set of natural number set N as time slot sets, such as $2^N = \{\emptyset, \{1\}, \{1, 2\}, \{1, 2, 3\}, \dots\}$. Let S be a set-cover for a time slot schedule. Let E be a directed edge set. Let S_i be a cover-set for a time slot i . Let $E(S_i)$

415 be the set of non-interfering edges in S_i . The optimization of
416 time slot allocation is as follows:

$$417 \quad S^* \leftarrow \arg \min_{S \in 2^N} |S|, \quad (2)$$

418 where $S = \{S_i | S_i \text{ is a cover-set for time slot } i\}$ and
419 $E = \bigcup_{S_i \in S} E(S_i)$.

420 For this optimization, we propose an STMAC Set-Cover
421 algorithm as shown in Algorithm 1. The optimization objective
422 of the STMAC Set-Cover algorithm is *to find a set-cover*
423 *with the minimum number of time slots, mapped to cover-sets.*
424 A schedule of cover-sets of which the edges are the concurrent
425 transmissions for a specific time slot can be represented as a
426 mapping from the set S of time slots S_i (*i.e.*, cover-sets) to
427 edges $e_j \in E$. A set-cover returned as S by Algorithm 1 might
428 not be optimal since the set-covering problem is originally
429 NP-hard. That is, STMAC Set-Cover is an extension of the
430 legacy Set-Cover [21], where families (*i.e.*, sets of elements)
431 are fixed. However, in our STMAC Set-Cover, the families are
432 not given, but should be dynamically constructed as cover-sets
433 during the mapping. Each cover-set S_i needs a time slot i ,
434 so one time slot is mapped to a cover-set that is a set of
435 non-interfering edges in G .

436 The lines 5-10 in Algorithm 1 show that the search
437 for a new maximum cover-set, which is a cover-set with
438 the maximum number of edges covered by a time slot,
439 is repeated until all the edges in E are covered by cover-
440 sets. Refer to Appendix B for the detailed description of
441 *Search_Max-Compatible_Cover_Set(G, E')* in line 6. The
442 time complexity of Algorithm 1 is $O(E \cdot V \cdot (V + E))$. Since
443 the number of vehicles at one intersection is still within a
444 reasonable bound, the time taken to calculate the optimal cover
445 set shall also be within a reasonable bound. The polynomial
446 time complexity of Algorithm 1 can be efficiently handled by
447 the edge-centric computing [18] in RSU.

Algorithm 1 STMAC-Set-Cover Algorithm

```

1: function STMAC_SET_COVER( $G$ ) ▷  $G$  is a
   line-of-collision (LoC) graph
2:    $E' \leftarrow G(E)$  ▷  $E'$  is the set of the remaining edges not
   belonging to any cover-set
3:    $S \leftarrow \emptyset$  ▷  $S$  is for a Set-Cover
4:    $i \leftarrow 1$ 
5:   while  $E' \neq \emptyset$  do
6:      $S_i \leftarrow \text{Search\_Max\_Compatible\_Cover\_Set}(G, E')$ 
       ▷ search for a Maximum Cover-Set for the remaining
       edges in  $E'$ 
7:      $E' \leftarrow E' - S_i$ 
8:      $S \leftarrow S \cup \{S_i\}$ 
9:      $i \leftarrow i + 1$ 
10:  end while
11:  return  $S$ 
12: end function

```

448 Fig. 6 shows an example of a search sequence for a set-cover
449 with maximum cover-sets by Algorithm 1. For the first time
450 slot, in Fig. 6, vertex 3 is selected as a start node for time slot
451 1 because it has the highest degree. Vertex 7 can also transmit

in time slot 1 since vertex 7 is not the receiver of vertex 3
and has a spatial disjoint feature. Next, vertexes 2 and 8 are
selected as the next transmitters. Through a similar procedure
for the remaining vehicles, 5 time slots can cover all the
transmissions for the LoC graph G instead of 8 time slots
for each vehicle. Thus, the mapping between time slot and
cover-set is constructed by the STMAC Set-Cover algorithm
for the transmission schedule.

Note that the STMAC Set-Cover algorithm can be extended
to consider an interference range existing in real radio com-
munications [29]. Algorithm 3 in Appendix B describes
for the STMAC Set-Cover considering the interference
range.

B. Contention Period Optimization

In this section, we explain the contention period optimiza-
tion for the efficient channel usage, considering the arrival
rate of unregistered vehicles to the communication range of
an RSU at an intersection. This adaptation is possible because
vehicles in an urban area move along the confined roadways,
so the arrival rate can be measured in vehicular networks
while such a measurement is not feasible in mobile ad hoc
networks due to free mobility. Note that the arrival rate can
be measured by several ways such that loop detectors installed
at intersections, object recognition in traffic cameras.

The contention period is dynamically adapted according to
the arrival rate of unregistered vehicles to the communication
range of an RSU. As the number of vehicles increases for
an RSU, the length of CFP in the superframe duration will
increase, since more vehicles should be allocated with their
time slots for channel access. Thus, the length of CP should
be determined according to the expected number of arriving,
unregistered vehicles in one superframe duration to enable the
vehicles the opportunity to be registered in the RSU with a
registration frame. If the CP length is too short, registration
frames toward the RSU will encounter many collisions during
registration attempts, and only a few vehicles can therefore
be registered. In contrast, if the CP length is too long, most
of the time in CP will be wasted after registering all arriving
vehicles in the RSU, resulting in a poor channel utilization.
Thus, we need to find the appropriate length of CP to guarantee
new incoming vehicles are given the opportunity to registered
with the RSU in a finite period of time (*e.g.*, one superframe
duration) within the same superframe.

Let λ_{jki} denote the vehicle arrival rate from an adjacent
intersection j_k to an intersection i , as shown in Fig. 3. Let λ
be the total arrival rate for the communication range of RSU
at intersection i per unit time (*e.g.*, 1 second) such that

$$\lambda = \sum_{k=1}^n \lambda_{jki}. \quad (3)$$

Here n is the number of neighbor intersections of inter-
section i . RSU at an intersection i observes the number of
vehicles that arrive within its transmission coverage from its
adjacent road segments. We can simply calculate λ with the
total arrivals of vehicles for all incoming road segments per
unit time.

506 We leverage the concept of the slotted ALOHA [30] and
 507 the Reservation-ALOHA (R-ALOHA) [31] for CP adaptation.
 508 The original R-ALOHA was designed for ad hoc networks
 509 to reduce collisions [32], whereas the CP in our scheme is
 510 designed for vehicle registration to reserve time slots in the
 511 next CFP. R-ALOHA provides nodes with time-based multiple
 512 channel access in a wireless link with a reasonable access
 513 efficiency (*i.e.*, channel utilization) [31]. In CP, since new
 514 comer vehicles to an intersection area try to register their
 515 mobility information into the RSU with a single registration
 516 frame, R-ALOHA can be used for the CP in STMAC. Let
 517 s be the time duration of one superframe duration including
 518 CP and CFP duration.

- 519 • An unregistered vehicle attempts to send its registration
520 frame with probability p .
- 521 • N vehicles attempt to be registered in RSU in this
522 superframe duration, such that $N = \lambda \cdot s$.
- 523 • The probability that one vehicle succeeds in registering
524 its transmission request for a slot among N vehicles is:

$$525 \quad g_N = N \cdot p \cdot (1 - p)^{N-1}. \quad (4)$$

526 For the CP duration, the total number of slots to register N
527 vehicles is:

$$528 \quad M = \sum_{i=N}^1 \frac{1}{g_i} = \sum_{i=N}^1 \frac{1}{i \cdot p \cdot (1 - p)^{i-1}}. \quad (5)$$

529 Appendix A provides the detailed derivation for this equation.
 530 For the efficient operation, the possible values of λ are
 531 mapped into a pair of the optimal channel access probability p
 532 and total slot number M in off-line processing. This pair of p
 533 and M for the current λ is announced to unregistered vehicles
 534 by an RSU through a timing advertisement frame (TAF), spec-
 535 ified in Section V. Note that although the RSUs are responsible
 536 for the vehicle registration and the cover-set calculations,
 537 they can handle these procedures because each RSU only
 538 manages one intersection at which the number of vehicles is
 539 still bounded to a reasonable level, even in rush-hours.

540 So far, we have described the proposed spatio-temporal
 541 coordination-based channel access scheme and the contention
 542 period optimization. In the next section, we will introduce a
 543 new hybrid MAC protocol to combine the merits of PCF and
 544 DCF modes based on the proposed channel access scheme and
 545 the contention period optimization.

546 V. SPATIO-TEMPORAL COORDINATION BASED 547 MEDIA ACCESS CONTROL PROTOCOL

548 STMAC is a hybrid MAC protocol that combines the PCF
 549 and DCF modes for efficient channel utilization and quick
 550 driving safety information exchange. The PCF mode is used
 551 to (i) register unregistered vehicles in an RSU with their
 552 mobility information, (ii) construct a collision-free channel
 553 access schedule for registered vehicles, and (iii) announce the
 554 channel access schedule for V2V communications in a similar
 555 way to that of WPCF [11]. In contrast, the DCF mode is used
 556 to enable the safety messages of the registered vehicles to be
 557 exchanged with other registered vehicles and without frame
 558 collision in V2V communications.

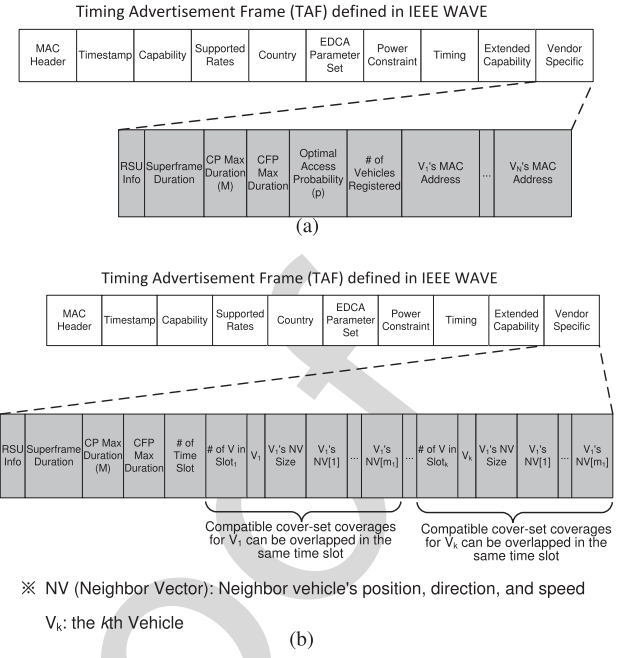


Fig. 7. Timing advertisement frame (TAF) formats in STMAC. (a) TAF in CP. (b) TAF in CFP.

559 In STMAC, an RSU periodically broadcasts a timing adver-
 560 tisement frame (TAF). The TAF is a beacon frame following
 561 the standard of the IEEE WAVE [33]. In STMAC, it has two
 562 formats, including TAF in CP and TAF in CFP as shown
 563 in Fig. 7. Both formats in the vendor specific field have some
 564 common fields, such as RSU information, superframe duration,
 565 CP max duration (*i.e.*, M), and CFP max duration. The vendor
 566 specific field of TAF for CP shown in Fig. 7(a) additionally
 567 contains optimal access probability (*i.e.*, p), the number of
 568 vehicles registered, and registered vehicles' MAC addresses.
 569 The vendor specific field of TAF for CFP in Fig. 7(b) con-
 570 tains other information, such as the number of time slots,
 571 the transmission schedule in each time slot, and the neighbor
 572 vectors (NV). NV contains the mobility information (*i.e.*, the
 573 current position, direction, and speed) of neighboring vehicles.

574 In STMAC, time is divided into superframe duration, and
 575 each superframe duration consists of two phases, the CP phase
 576 and CFP phase, as shown in Fig. 8. These two phases are
 577 explained in the following subsections.

578 A. CP Phase for Vehicle Registration

579 In the CP phase, unregistered vehicles attempt to be reg-
 580 istered in an RSU based on contention. Fig. 8(a) shows
 581 a contention-period time sequence for vehicle registration.
 582 As shown in Fig. 8(a), a TAF at the beginning of a CP is firstly
 583 transmitted by an RSU in a DSRC control channel (CCH),
 584 after a DCF inter frame space (DIFS) period, indicating the
 585 start of a contention period.

586 The TAF mainly contains a list of the registered vehicles
 587 and the RSU's service channel number (SCH#) in the RSU
 588 Info part as shown in Fig. 7(a). Next, after receiving the TAF,
 589 the vehicles start contending the transmission opportunity to
 590 send a registration request (*i.e.*, REQ in Fig. 8(a)). It is possible

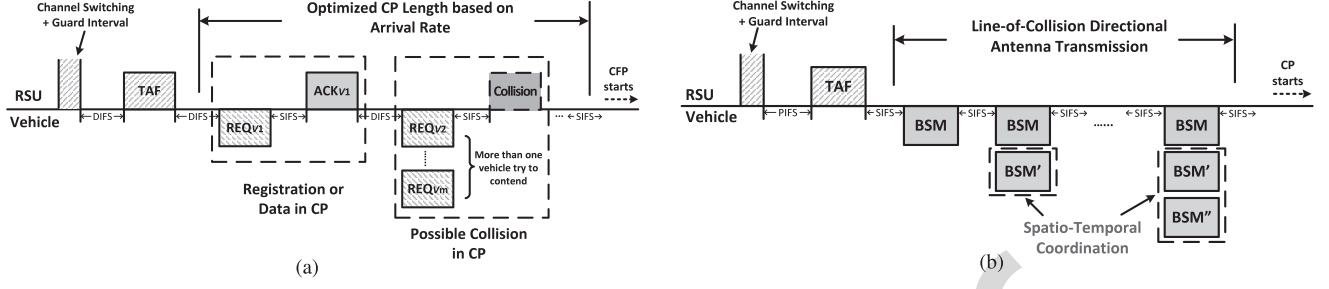


Fig. 8. Time sequence in STMAC protocol. (a) Contention-period time sequence. (b) Contention-free-period time sequence.

591 that multiple vehicles attempt to contend, causing a collision
 592 at the RSU. After this contention period, the contention free
 593 period starts and all registered vehicles (including newly reg-
 594 istered vehicles) switch their CCH channel to an SCH channel
 595 specified in the TAF.

596 Let O_c be the number of vehicles that send packets, then
 597 the maximum CP length can be calculated as follows:

$$598 T_{CP}^{STMAC} = DIFS + TAF + (DIFS + REQ + SIFS + ACK) \\
 599 \cdot \sum_{i=O_c}^1 \frac{1}{i \cdot p \cdot (1-p)^{i-1}} + SIFS + T_{CS} + T_{GI}, \\
 600 \quad (6)$$

601 where $DIFS$, TAF , REQ , $SIFS$, ACK , T_{CS} , and T_{GI} are
 602 the time for the DCF inter frame space, the timing adver-
 603 tisement frame, the registration request frame, the short inter
 604 frame space, the acknowledgement frame, the channel switch,
 605 and the guard interval, respectively, and $\sum_{i=O_c}^1 \frac{1}{i \cdot p \cdot (1-p)^{i-1}}$
 606 is the expected number of vehicle registrations derived
 607 in Section IV-B.

608 Note that during the CP phase, both registered and unregis-
 609 tered vehicles can transmit an emergency message to an RSU
 610 for emergency data dissemination (e.g., an accident).

611 B. CFP Phase for Driving Information Exchange

612 In a CFP phase, registered vehicles attempt exchange their
 613 driving safety information with their neighboring vehicles
 614 based on the contention-free schedule in service chan-
 615 nels (SCHs). As shown in Fig. 8(b), a TAF containing the
 616 channel access schedule of registered vehicles is broadcasted
 617 by an RSU. Each vehicle based on the schedule in the TAF
 618 transmits its basic safety message (BSM) (e.g., mobility infor-
 619 mation and vehicle internal states) to its intended receivers for
 620 the time slot. As shown in the dashed line box of Fig. 8(b),
 621 the transmissions of BSM packets are multiplexed in the time
 622 slots according to the spatio-temporal coordination described
 623 in Section IV-A. Let O_r^{STMAC} be the number of time slots
 624 allocated by the spatio-temporal coordination in a CFP; then,
 625 O_c vehicles may use O_r^{STMAC} time slots to exchange safety
 626 messages. Thus, the maximum length of a CFP in STMAC
 627 can be expressed as:

$$628 T_{CFP}^{STMAC} = PIFS + TAF + \sum_{i=1}^{O_r^{STMAC}} (SIFS + BSM_i) \\
 629 + SIFS + T_{CS} + T_{GI}, \quad (7)$$

630 where $PIFS$ and BSM_i are the time for the PCF interframe
 631 space and the basic safety message for vehicle i , respectively.

632 Using the NVs from the TAF, each vehicle i constructs the
 633 coverage regions for its intended transmissions by the direc-
 634 tional antenna and the transmission power control. Note that
 635 during the CFP phase, if the RSU has an emergency message,
 636 it can announce a TAF having emergency information.

637 Thus, by the CP and CFP phases, STMAC can allow for
 638 not only the fast exchange of driving safety information among
 639 vehicles, but also the fast dissemination of emergency data of
 640 the vehicles under the RSU.

641 C. Vehicle Mobility Information Update

642 In the STMAC protocol, the RSU periodically broadcasts
 643 a special TAF in a CP phase to collect the most current
 644 mobility information of all registered vehicles. This enables
 645 vehicles to correctly select the transmission direction and
 646 power control parameters by the latest position of a receiver
 647 vehicle. This TAF is also used to deregister vehicles that
 648 have left the communication range of the RSU, and which
 649 do not respond to this TAF. Each registered vehicle sends
 650 its updated mobility by transmitting a BSM, which includes
 651 its mobility information, to the RSU. The superframe for the
 652 vehicle mobility information update is repeated every U times,
 653 such as $U = 10$, considering the mobility prediction accuracy.
 654 With this update, the RSU estimates the vehicle's mobility
 655 in the near future (e.g., after 100 milliseconds) for time slot
 656 scheduling.

657 D. Performance Analysis

658 We have so far explained the design of STMAC protocol.
 659 Now we analyze the performance of STMAC and WPCF.
 660 Since WPCF is the MAC protocol most similar to STMAC,
 661 we particularly study the performance of WPCF. Table I
 662 shows the performance analysis of STMAC and WPCF. The
 663 maximum CP and CFP lengths of STMAC were discussed
 664 in Sections V-A and V-B. Notice that the number of time
 665 slots (i.e., O_r^{STMAC}) allocated in a CFP of STMAC is a result
 666 of the spatio-temporal coordination. The acknowledgement
 667 process between any two LoC vehicles, of which the time
 668 is $SIFS + ACK$, is removed to improve the efficiency of the
 669 safety information exchange. We assume that every vehicle has
 670 safety messages that must be sent. The superframe duration
 671 of STMAC can be described as

$$672 T_{SF}^{STMAC} = T_{CP}^{STMAC} + T_{CFP}^{STMAC}. \quad (8)$$

TABLE I
 PERFORMANCE ANALYSIS OF STMAC AND WPCF

Scheme	Maximum CP Length (T_{CP})	Maximum CFP Length (T_{CFP})
STMAC	$DIFS + TAF + (DIFS + REQ + SIFS + ACK) \cdot \sum_{i=O_c}^1 \frac{1}{i \cdot p \cdot (1-p)^{i-1}} + SIFS + T_{CS} + T_{GI}$	$PIFS + TAF + \sum_{i=1}^{O_r^{STMAC}} (SIFS + BSM_i) + SIFS + T_{CS} + T_{GI}$
WPCF [11]	$DIFS + TAF + (DIFS + REQ + SIFS + ACK) \cdot \sum_{i=O_c}^1 \frac{1}{i \cdot p \cdot (1-p)^{i-1}} + SIFS + END$	$SIFS + TAF + \sum_{i=1}^{O_r} (WPIFS[1] + BSM_i + SIFS + ACK) + END$

673 The maximum CP length T_{CP}^{WPCF} of WPCF is similar to
 674 that of STMAC, but WPCF has no registration mechanism
 675 for continuous communications, which means that whenever
 676 a vehicle has a packet to send, it needs to reserve a time slot
 677 in a CP. Also, the vehicles with the WPCF scheme, which
 678 reserved the time slots in the CP, do not utilize the spatial
 679 feature to reduce the number of time slots. Thus, the maximum
 680 CFP length of WPCF is determined by the number of vehicles
 681 with reserved time slots in the CP. Note that the number of
 682 vehicles within the coverage of one RSU at an intersection is
 683 a reasonable number, the CFP period will increase reasonably
 684 as the number of vehicles increases. Assume that there are O_r
 685 vehicles having packets to send; the maximum CFP length for
 686 these O_r vehicles is:

$$687 T_{CFP}^{WPCF} = SIFS + TAF + \sum_{i=1}^{O_r} \times (WPIFS[1] + BSM_i + SIFS + ACK) + END, \quad (9)$$

690 where $WPIFS$ is the WAVE PCF inter frame space defined
 691 in WPCF [11]; $WPIFS[k] = SIFS + (k \times T_{slot})$; k is the
 692 sequence number for the transmission order of a vehicle in the
 693 current CFP schedule, and k is always 1 because every reg-
 694 istered vehicle transmits its data frame to the RSU according
 695 to its transmission order in the schedule [11]; BSM_i is the
 696 transmission time of the basic safety message for a vehicle i ;
 697 and END is the CFP end frame sent by an RSU, which can
 698 be equal to the $T_{CS} + T_{GI}$ of STMAC. Thus, the superframe
 699 duration T_{SF}^{WPCF} of WPCF is

$$700 T_{SF}^{WPCF} = T_{CP}^{WPCF} + T_{CFP}^{WPCF}. \quad (10)$$

701 To measure the interval between two consecutive safety
 702 messages which are transmitted by a vehicle and are received
 703 by its neighboring vehicles, we define E2E delay to describe
 704 it. Based on the superframe duration of STMAC and WPCF,
 705 the E2E delay of STMAC (denoted as T_{E2E}^{STMAC}) and that of
 706 WPCF (denoted as T_{E2E}^{WPCF}) can be estimated by the uniformly
 707 distributed channel access in both CP and CFP phases:

$$708 T_{E2E}^{STMAC} = \frac{T_{CFP}^{STMAC}}{2} + T_{CP}^{STMAC} + \frac{T_{CP}^{STMAC}}{2}$$

$$709 = \frac{T_{SF}^{STMAC}}{2} + T_{CP}^{STMAC}. \quad (11)$$

$$710 T_{E2E}^{WPCF} = \frac{T_{CFP}^{WPCF}}{2} + T_{CP}^{WPCF} + \frac{T_{CP}^{WPCF}}{2}$$

$$711 = \frac{T_{SF}^{WPCF}}{2} + T_{CP}^{WPCF}. \quad (12)$$

 TABLE II
 PARAMETERS FOR PERFORMANCE ANALYSIS

Parameter	Value
T_{slot}	13 μs
SIFS	32 μs
PIFS	45 μs (SIFS + T_{slot})
DIFS	58 μs (SIFS + $T_{slot} \times 2$)
$T_{CS} + T_{GI}$ (END)	4 ms
Data rate	6 Mbps
Size of TAF packet	800 bit + Payload
Size of BSM packet	1024 bit + 88 bit
Size of REQ packet	288 bit
Size of ACK packet	128 bit

712 We verified the analytical models of STMAC and WPCF
 713 by comparing the analytical results with the simulation results
 714 in Section VI-B based on the parameters in Table II. Note that
 715 the contents of a BSM can be modified to adapt to different
 716 scenarios, which may vary the size of a BSM.

717 Since it is a CSMA/CA-based MAC scheme, LMA does
 718 not have the concept of superframe. Thus, we cannot deter-
 719 mine the superframe duration as we can for STMAC and
 720 WPCF. Note that many analysis models have been proposed
 721 (e.g., Markov chain model [34]–[37]) to describe the perfor-
 722 mance of CSMA/CA schemes.

723 So far, we have explained the design of the STMAC
 724 protocol. In the next section, we will evaluate our STMAC
 725 with baselines in realistic settings.

726 VI. PERFORMANCE EVALUATION

727 In this section, we evaluate the performance of STMAC
 728 in terms of average superframe duration, E2E delay, and
 729 packet loss ratio as performance metrics. We set the data
 730 rate as 6 Mbps, and utilize the Nakagami-3 [27] radio model
 731 for both transmitter and receiver to support the irregularity of
 732 transmission coverage, interference, and path loss in vehicular
 733 environments. We assume that a transmission coverage can be
 734 optimized in STMAC from a design perspective for an opti-
 735 mized communication coverage. Also, multiple transmissions
 736 can be emitted toward multiple receivers by a transmitter's
 737 directional antenna.

738 The evaluation settings are as follows:

- 739 • **Performance Metrics:** We use (i) *Average superframe*
 740 *duration*, (ii) *E2E delay*, and (iii) *Packet loss ratio* as
 741 metrics for the performance.
- 742 • **Baseline:** LMA [10], WPCF [11], DMMAC [14], and
 743 EDCA [4] were used as baselines.

TABLE III
SIMULATION CONFIGURATION

Parameter	Description
Road network	The number of intersections is 11. The area of the road map is $500 \text{ m} \times 600 \text{ m}$ (<i>i.e.</i> , $0.31 \text{ miles} \times 0.37 \text{ miles}$).
Number of vehicles (N)	The number of vehicles moving in the road network ranges from 50 to 300. The default is 150.
Communication range (R)	$R = 25 \sim 150 \text{ meters}$ (<i>i.e.</i> , $82.02 \sim 492.13 \text{ feet}$). The default is 75 meters.
GPS location error (ϵ)	$\epsilon = 0 \sim 18 \text{ meters}$ (<i>i.e.</i> , $0 \sim 59 \text{ feet}$). The default is 3 meters.
Maximum vehicle speed (v_{max})	Maximum vehicle speed (<i>i.e.</i> , speed limit) for road segments. The default is 22.22 m/s (<i>i.e.</i> , 49.7 MPH).
Radio delay (d_r)	The time taken to switch from Rx to Tx mode for OFDM PHY defined in IEEE 802.11-2012 [4]. The default is $1 \mu\text{s}$.
Transmission power (P)	The value is variable, decided by equation (1) and Algorithm 1
Data traffic rate	The frequency of safety information transmission. The default is 100 packets per second.

- **Parameters:** For the performance, we investigate the impacts of the following parameters: (i) *Vehicle number* (*i.e.*, Vehicle traffic density) N , (ii) *GPS position error* (*i.e.*, Vehicle location error) ϵ , (iii) *Radio antenna*, and (iv) *Contention period duration*.

We use a road network with 11 intersections associated with 11 RSUs from a rectangular area of Los Angeles, CA, U.S.A. using Open Street Map [38] as shown in Fig. 9. The total length of the road segments of the road network is about 4.92 km (*i.e.*, 3.06 miles). We built STMAC, WPCF, LMA, and DMMAC using OMNeT++ [39] and Veins [40] as well as applying the settings specified in Table III. Veins is an open source software to simulate vehicle communication and networks, including signal fading models. Directional antenna coverage is formed by a directional antenna array [23] on top of a realistic wireless radio model in Veins, such as Nakagami fading model [27]. To use realistic vehicle mobility in the road network, we fed the vehicle mobility information to OMNeT++ using a vehicle mobility simulator called SUMO [41] via the TraCI protocol [41]. SUMO was extended such that vehicles move around, rather than escape from a target road network.

Because our objective is to show the performance of local communications among RSU and vehicles in the same road segment, rather than the E2E delivery delay between two remote vehicles in a large-scale road network, the simulation topology shown in Fig. 9 is sufficient for evaluating our proposed protocol. The packets for safety messages continue to be generated during the travel of vehicles. We averaged 10 samples with confidence interval (*i.e.*, error bar) in the performance results.

A. Comparison of Data Delivery Behaviors

We compared the data delivery behaviors of STMAC, WPCF, LMA, DMMAC, and EDCA with the cumulative distribution function (CDF) of the superframe duration,

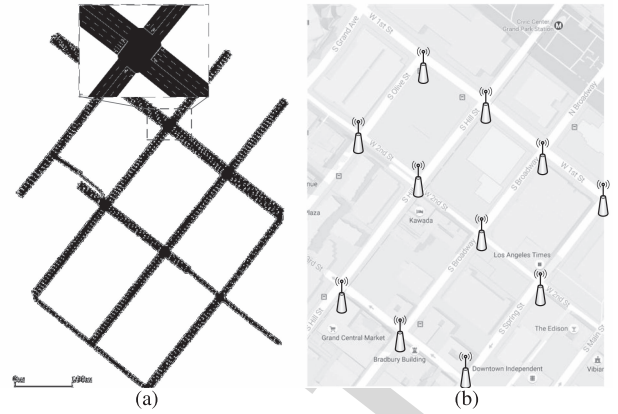


Fig. 9. Road network for simulation. (a) Extracted map in SUMO. (b) Real map with RSU placement.

E2E delay, and packet loss ratio. Fig. 10 shows that the CDF of STMAC reaches 100% much faster than those of WPCF, LMA, DMMAC, and EDCA. For example, STMAC has the average superframe duration of 0.021 s for 80% CDF, while for the same CDF value, WPCF has that of 0.052 s . Also, STMAC has the E2E delay of 0.017 s for 80% CDF while WPCF has that of 0.055 s and LMA has that of 1.2 s . In addition, The packet loss ratio of STMAC is 0.3% for 80% CDF. While that for WPCF is 25% and that for LMA is 1.8%. We observed that STMAC has better channel utilization, shorter E2E delay, and less packet loss ratio than WPCF, LMA, DMMAC, and EDCA. We show the forwarding performance of these three schemes quantitatively in the following subsections.

B. Impact of Number of Vehicles

To examine the impact of the vehicle density, we varied the number of vehicles from 50 to 300 in the simulations. Since LMA, DMMAC, and EDCA do not have a superframe period, we only verified the analytical results of superframe duration and E2E delay of STMAC and WPCF.

Fig. 11(a) shows both the analytical and simulation results of the average superframe duration for the different vehicle densities. We obtained the analytical results from the analysis in Section V-D by uniformly assigning vehicles to each RSU. Note that the setting of uniformly distributed vehicles is used to get the performance results of the theoretical analysis in Section V-D. In the simulation, the vehicles are not uniformly distributed. The vehicle traffic is from SUMO which models a realistic vehicle mobility. Vehicles select their random destination and move to the destination in a shortest path. The results in Fig. 11(a) show that the simulation data match well with the analytical results. The average superframe duration of STMAC is shorter than that of WPCF. Especially, in a highly congested road situation, STMAC outperforms WPCF by 66.7%. It was observed that when the vehicle density increases, a small gap appears between the simulation and the analytical data of WPCF. This is due to the non-uniform vehicle distribution in the simulation. A small gap between the simulation result and analytical result of STMAC is also observed, but due to

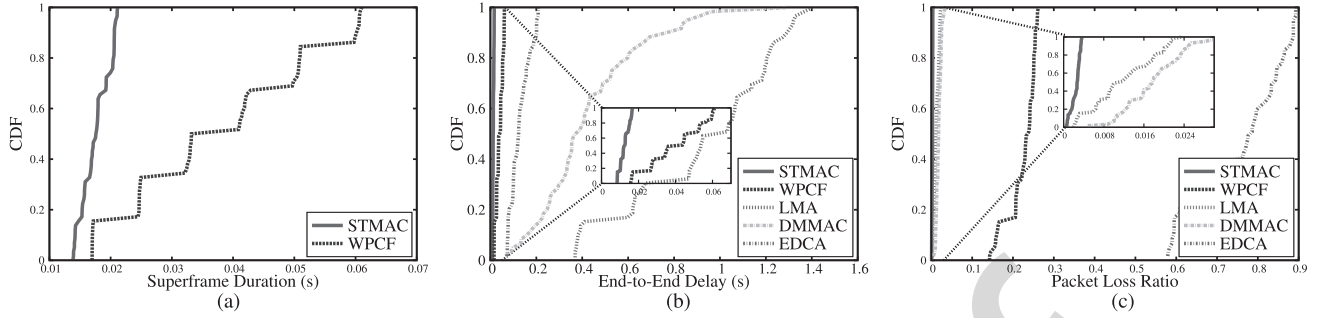


Fig. 10. CDF of superframe duration, E2E delay and packet loss ratio for STMAC, WPCF, and LMA. (a) CDF of superframe duration. (b) CDF of E2E delay. (c) CDF of packet loss ratio.

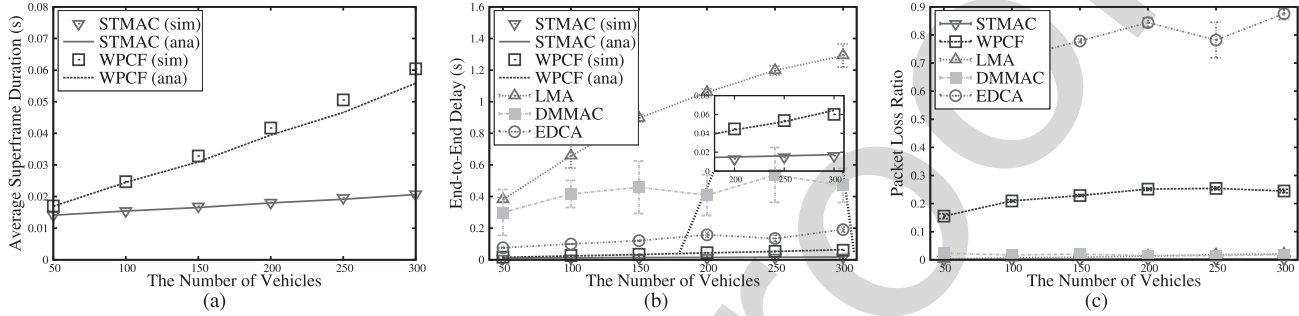


Fig. 11. Impact of the number of vehicles. (a) Average superframe duration for STMAC and WPCF. (b) Packet E2E delay for STMAC, WPCF, and LMA. (c) Packet loss ratio for STMAC, WPCF, and LMA.

818 the scale of the figure, such a gap is not significant. Notice
 819 that in Fig. 11(a), the curve of STMAC is linearly increasing
 820 rather than constant according to the increase of vehicles.
 821 Also, note that the average superframe duration determines
 822 the time duration of a vehicles safety information transmission
 823 toward its adjacent vehicles in the LoC graph. Thus, the shorter
 824 average superframe duration indicates the more often exchange
 825 of safety information among vehicles.

826 As described in Section V-D, the average superframe duration
 827 determines the packet E2E delay. Fig. 11(b) shows the
 828 analytical and simulation results of the average E2E delay of
 829 packet delivery. Overall, the simulation results show a good
 830 agreement with the analytical results, as shown in the small
 831 window of Fig. 11(b). As the number of vehicles increases,
 832 all of STMAC, WPCF, LMA, DMMAC, and EDCA have
 833 a longer average E2E delay. In any road traffic condition
 834 (*i.e.*, $N = 50$ through $N = 300$), STMAC has a shorter packet
 835 E2E delay than WPCF, LMA, DMMAC, and EDCA due to
 836 both the optimized CP duration and concurrent transmissions
 837 by spatio-temporal coordination. Especially, for highly con-
 838 gested road traffic of $N = 300$, the packet E2E delay of
 839 STMAC is one third that of WPCF. Notice that the E2E
 840 delay of LMA is identical to that in the results reported in
 841 LMA [10]. LMA has much higher E2E delays than those of
 842 STMAC and WPCF in all vehicle densities. This is due to the
 843 mechanism of Carrier Sense Multiple Access with Collision
 844 Avoidance (CSMA/CA) [4] that can let multiple control frames
 845 experience collision before the transmission of a data frame.

846 Fig. 11(c) shows the packet loss ratio according to the
 847 increasing number of vehicles. In all vehicle densities from

50 to 300, STMAC has a much lower packet loss ratio than
 both WPCF, LMA, DMMAC, and EDCA since in STMAC,
 vehicles can communicate with their LoC vehicles by an
 optimized communication range. Even for highly congested
 road traffic of $N = 300$, STMAC gains a packet loss ratio less
 than 1%, but for the packet loss ratio of WPCF and LMA are
 24% and 2.5%, respectively. Through the observation of the
 simulations, the high packet loss ratio of WPCF is caused by
 signal attenuation and the packet collisions in handover areas.
 The packet loss of LMA, which lacks spatial coordination,
 is produced mainly by the packet collisions between the data
 frames and the control frames. The spatial coordination and
 the transmission power control induce a very low packet loss
 ratio for STMAC.

From the performance comparison of the superframe duration,
 the E2E delay, and the packet loss ratio, STMAC
 outperforms the other state-of-the-art schemes considerably,
 indicating that it can support reliable and fast safety message
 exchange. These improvements are because that STMAC
 allows vehicles to transmit their safety information frames
 with their neighboring vehicles in the LoC graph through
 spatio-temporal coordination in an RSU in a direct V2V com-
 munication. This coordination can reduce the frame collision
 and the direct V2V communication reduces the data delivery
 between vehicles. On the other hand, LMA lets vehicles
 access the wireless channel randomly, so this increases the
 frame collision probability as the number of vehicles increases.
 Also, since WPCF does not consider CP duration optimization
 unlike STMAC, the channel utilization of WPCF is worse than
 that of STMAC.

848
849
850
851
852
853
854
855
856
857
858
859
860
861
862
863
864
865
866
867
868
869
870
871
872
873
874
875
876
877

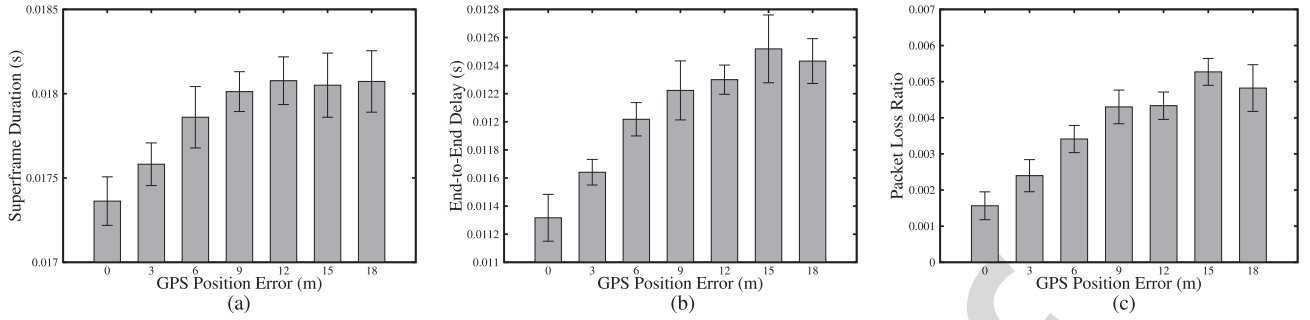


Fig. 12. Impact of GPS position error. (a) Average superframe duration. (b) Packet E2E delay. (c) Packet loss ratio.

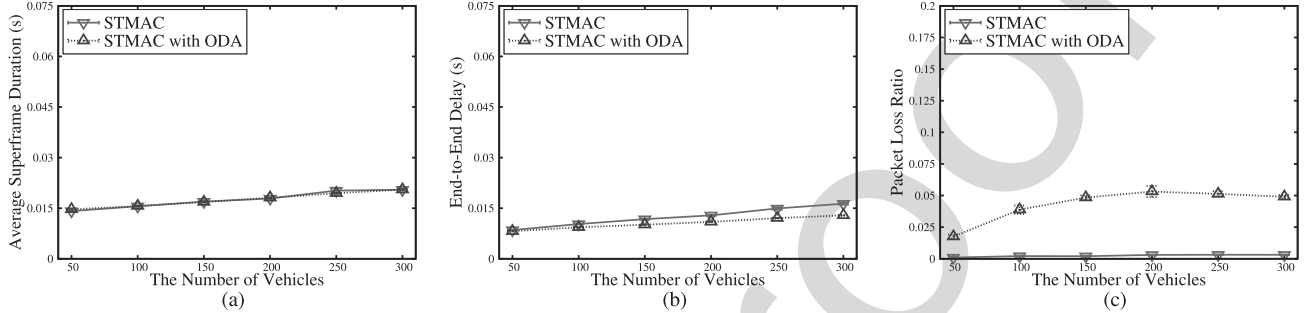


Fig. 13. Impact of radio antenna. (a) Average superframe duration with omni-directional antenna. (b) Packet E2E delay with omni-directional antenna. (c) Packet loss ratio with omni-directional antenna.

C. Impact of GPS Position Error

In an urban area, tall buildings usually seriously affect the precision of GPS localization, which can also influence the performance of STMAC since STMAC utilizes the coordinates of vehicles to schedule time slots. Therefore, we evaluated the performance of STMAC by varying the GPS position error at a medium vehicle density (*i.e.*, 150 vehicles). Fig. 12 shows the average superframe duration, E2E delay, and packet loss ratio according to GPS position error. The average superframe duration of STMAC increases when the GPS error increases, as shown in Fig. 12(a), but when the error reaches above 9 meters, the average superframe duration remains stable. The worst case occurred at the GPS position error with 12 meters, where the average superframe duration is about 18.1 *ms*, which is still within a safe driving range (*e.g.*, 100 *ms* [42]). On the other hand, as the GPS error increases, the E2E delay also increases as shown in Fig. 12(b), and the worst case is about 12.5 *ms* on average. For packet loss ratio, in the zero GPS position error, STMAC performs with less than 0.18% packet loss ratio, and gains increased packet loss ratio as the GPS error range increases. From the result shown in this figure, it is expected that STMAC can work well for safety message exchange [42] even in urban road networks with a high GPS error due to buildings. The good tolerance of GPS error in STMAC benefits from the design of STMAC protocol. Algorithm 1 considers the GPS error when using the vehicles position information to schedule the transmissions. Based on the algorithm, vehicles transmit data following the enlarged transmission range to compensate the impact of GPS error.

D. Impact of Radio Antenna

To evaluate the impact of radio antenna, we conducted simulations by switching the radio antenna. Fig. 13 shows the impact of radio antenna, such as directional antenna and omnidirectional antenna (ODA). As shown in Fig. 13(a), STMAC using directional antenna has almost the same superframe duration as that of STMAC using ODA. For packet E2E delay, as shown in Fig. 13(b), STMAC using directional antenna has slightly longer E2E delay than STMAC using ODA. This is because vehicles using ODA in STMAC exchange safety messages with adjacent vehicles when updating their mobility information to RSUs; this update reduces the E2E delay of safety messages.

For data packet loss ratio, as shown in Fig. 13(c), the data packet loss ratio of STMAC when using the directional antenna is less than that of STMAC when using ODA. The data packet loss when using ODA is due to two factors: signal attenuation and the packet loss in handover areas. The packet loss in handover areas results from the channel switch of vehicles in the handover areas. Assume that vehicle A (V_A) that is moving into a handover area becomes registered in a new RSU (RSU_n) and its service channel is switched according to RSU_n . The predecessor RSU (RSU_p) of V_A can still generate transmission schedules including V_A until the next update period. The other vehicles in RSU_p receiving the schedules can transmit their data packets to V_A in the handover area, although V_A has switched from the service channel of RSU_p to the service channel of RSU_n . The vehicles with ODA in RSU_p can increase the data packet loss in the handover areas, since V_A in the handover area can receive

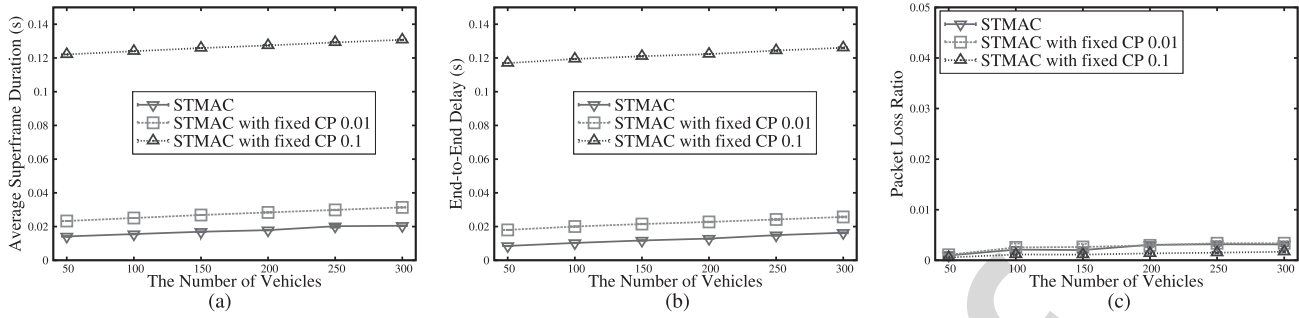


Fig. 14. Impact of contention period duration. (a) Average superframe duration for CP duration. (b) Packet E2E delay for CP duration. (c) Packet loss ratio for CP duration.

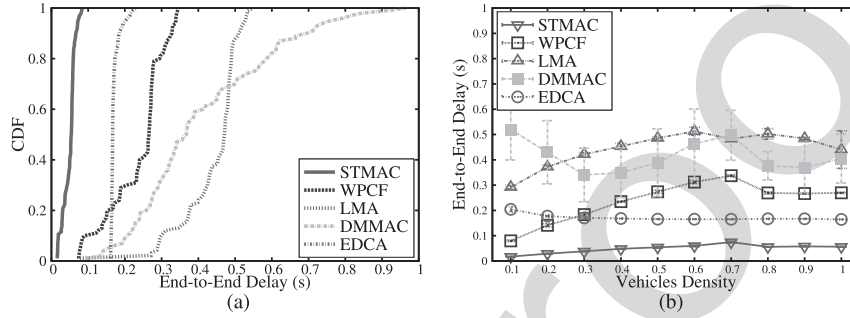


Fig. 15. Performance in highly congested scenario. (a) CDF of E2E delay at one intersection. (b) Packet E2E delay at one intersection.

938 more data packets from the vehicles with ODA than from the
 939 vehicles with directional antenna. However, this data packet
 940 loss does not affect the average packet E2E delay, because the
 941 vehicles in handover areas can receive data packet correctly
 942 from the other vehicles in the coverage of RSU_n , as shown
 943 in Fig. 13(b).

944 The results in Fig. 13 indicate that STMAC with directional
 945 antenna can significantly reduce packet loss while maintaining
 946 a good packet E2E delay in comparison with STMAC with
 947 omni-directional antenna.

948 *E. Impact of Contention Period Duration*

949 We also fixed the length of the CP to show the impact of
 950 the contention period duration. Particularly, we select 100 ms
 951 and 10 ms for the fixed-length CP to evaluate the performance
 952 of STMAC with the CP adaptation. Fig. 14 shows the impact
 953 of CP duration in STMAC. For average superframe duration,
 954 as shown in Fig. 14(a), the E2E delay of STMAC with
 955 CP adaptation has shorter average superframe duration than
 956 STMAC with constant CP duration (*i.e.*, 0.01s and 0.1 s,
 957 respectively). For packet E2E delay with CP adaptation,
 958 as shown in Fig. 14(b), the E2E delay of STMAC with CP
 959 adaptation is shorter than STMAC with both constant CP
 960 durations. For packet loss ratio with CP adaptation, as shown
 961 in Fig. 14(c), STMAC has small packet loss regardless of
 962 CP adaptation. This small packet loss ratio benefits from the
 963 directional antenna that reduces packet collisions.

964 *F. Performance in Highly Congested Scenario*

965 To measure the scalability of STMAC, we performed a
 966 simulation in a highly congested scenario at one intersection

with four road segments. The intersection has three lanes
 967 on each road segment, and the length of each road seg-
 968 ment is 300 meters. An RSU is placed at the intersection.
 969 Consider a vehicle with 5 meters length, and the minimum
 970 gap between two vehicles is 2.5 meters. To fully occupy the
 971 intersection, about 922 vehicles are required at the intersection.
 972 Fig. 15 shows the E2E delay performance among STMAC,
 973 WPCF, LMA, DMMAC, and EDCA. STMAC obtained the
 974 best performance on the E2E delay, which shows that the
 975 scalability of STMAC is good. In Fig. 15(a), the packet E2E
 976 delays in STMAC are always within 100 ms even in the full
 977 congested scenario, which can fulfill the minimum requirement
 978 for driving safety information exchange. Fig. 15(b) shows the
 979 trend of the packet E2E delay from a low density to a high
 980 density. With the increase of vehicles density, the packet E2E
 981 delays in STMAC, WPCF, and LMA also increase. The packet
 982 E2E delay in STMAC is much lower than that of WPCF and
 983 LMA, which is gained by the enhanced set-cover algorithm
 984 and the new hybrid MAC protocol utilizing the spatio-temporal
 985 coordination. Also, notice that the E2E delays in STMAC
 986 and WPCF reach the highest point at the vehicles density
 987 with 0.7. After the peak, the E2E delay maintains as almost
 988 constant. Based on the observation, the peak indicates the
 989 saturation scenario within the coverage of the RSU. When
 990 vehicles density is larger than 0.7, the intersection experiences
 991 traffic jam that hinders vehicles to move into the coverage of
 992 the RSU, which reduces the E2E delay.
 993

Therefore, the results from the performance evaluation show
 994 that STMAC is a promising MAC protocol for driving safety
 995 to support the reliable and rapid exchange of safety messages
 996 among nearby vehicles.
 997

VII. CONCLUSION

In this paper, we propose a Spatio-Temporal Coordination based Media Access Control (STMAC) protocol in an urban area for an optimized wireless channel access. We characterize the spatio-temporal feature using a line-of-collision (LoC) graph. With this spatio-temporal coordination, STMAC organizes vehicles that transmit safety messages to their neighboring vehicles reliably and rapidly. Vehicles access wireless channels in STMAC, combining the merits of the PCF and DCF modes. In the PCF mode, the vehicles register their mobility information in RSU for time slot reservation, and they then receive their channel access time slots from a beacon frame transmitted by an RSU. In the DCF mode, the vehicles concurrently transmit their safety messages to their neighboring vehicles through the spatio-temporal coordination. We theoretically analyzed the performance of STMAC, and conducted extensive simulations to verify the analysis. The results show that STMAC outperforms the legacy MAC protocols using either PCF or DCF mode even in a highly congested road traffic condition. Thus, through STMAC, a new perspective for designing a MAC protocol for driving safety in vehicular environments is demonstrated.

For future work, we will extend our STMAC to support data services (e.g., multimedia streaming and interactive video call) for high data throughput rather than for short packet delivery time. Also, we will study a traffic-light-free communication protocol for autonomous vehicles passing intersection without the coordination of a traffic light. For a highway scenario, we will study an efficient communication protocol for driving safety.

APPENDIX A
CONTENTION PERIOD ADAPTATION

For a particular number of vehicles N , we can find an optimal p that can give the best successful probability g_N for each vehicle to send a registration request, so through

$$\frac{dg_N}{dp} = N \cdot (1-p)^{N-1} - N \cdot (N-1) \cdot p \cdot (1-p)^{N-2} = 0, \quad (13)$$

we can obtain an optimal p :

$$p = \frac{1}{N}. \quad (14)$$

Accordingly, the optimal g_N is:

$$g_N = \left(1 - \frac{1}{N}\right)^{N-1}. \quad (15)$$

The average number of slots to register one vehicle among N vehicles based on Equation (4) is:

$$M_N = \frac{1}{g_N} = \frac{1}{N \cdot p \cdot (1-p)^{N-1}}. \quad (16)$$

After a vehicle is registered with M_N , M_{N-1} for only $N-1$ vehicles is computed in the same way:

$$M_{N-1} = \frac{1}{g_{N-1}} = \frac{1}{(N-1) \cdot p \cdot (1-p)^{N-2}}. \quad (17)$$

Therefore, the total number of slot to register N vehicles is:

$$M = \sum_{i=N}^1 \frac{1}{g_i} = \sum_{i=N}^1 \frac{1}{i \cdot p \cdot (1-p)^{i-1}}. \quad (18)$$

APPENDIX B

MAXIMUM COMPATIBLE SET ALGORITHM

To construct a set-cover, the STMAC-Set-Cover algorithm in Algorithm 1 searches for a maximum compatible cover-set, using *Search_Max-Compatible-Cover-Set*(G, E') with the LoC graph G and the edge set E' in Algorithm 2. The remaining edges of this edge set E' are used for further compatible cover-sets for concurrent communications in G .

Algorithm 2 Search-Max-Compatible-Cover-Set Algorithm

```

1: function SEARCH_MAX_COMPATIBLE_COVER_SET
   ( $G, E'$ ) ▷  $G$  is the LoC graph and  $E'$  is the set of the
   remaining edges not belonging to any cover-set
2:  $V' \leftarrow \emptyset$  ▷  $V' (\subseteq V)$  is for a set of vertices with
   directed edges in  $E'$  and initialized with  $\emptyset$ 
3:  $M_{max} \leftarrow \emptyset$  ▷  $M_{max}$  is for a maximum compatible
   cover-set and initialized with zero
4: for all edges  $e_{i,j} \in E'$  do
5:    $V' \leftarrow V' \cup \{v_i, v_j\}$ 
6: end for
7: for each vertex  $s \in V'$  do
8:    $M \leftarrow Make\_Maximal\_Compatible\_Set(G, V', E', s)$ 
9:   if  $|M_{max}| < |M|$  then
10:     $M_{max} \leftarrow M$ 
11:   end if
12: end for
13: return  $M_{max}$ 
14: end function

```

Algorithm 2 searches for a maximum compatible cover-set among maximal compatible cover-sets constructed by *Make_Maximal-Compatible-Set*(G, V', E', s) in Algorithm 3. Algorithm 2 takes as input E' that is a set of edges not belonging to any compatible cover-set and it returns the maximum compatible cover-set, M_{max} . V' is for a set of vertices with directed edges in E' . Lines 2-3 initialize the V' and M_{max} to \emptyset . In lines 4-6, V' is a set of vertices such that v_i and v_j are linked with any directed edges $e_{i,j}$ in E' . For each vertex s in V' as a start node (i.e., root vertex) for breadth-first search (BFS) [21], we find a candidate maximal compatible set, M . In lines 7-12, if the number of elements in M is bigger than that of M_{max} , M is set to M_{max} . After running the for-loop in lines 7-12, consequently, M_{max} is returned as a maximum compatible cover set for the given edge set E' .

Algorithm 3 computes a maximal compatible cover set with s as a starting vertex for BFS along with interference range. The input parameters in Algorithm 3 are G as the LoC graph, V' as the set of vertices for the remaining edges in E' , E' as the remaining edge set, and s as a start node for BFS in the subgraph corresponding to $G(V', E')$.

Algorithm 3 Make-Maximal-Compatible-Set Algorithm

```

1: function MAKE_MAXIMAL_COMPATIBLE_SET
   ( $G, V', E', s$ )  $\triangleright G$  is the LoC graph,  $V'$  is the set of
   vertices with directed edges in  $E'$ ,  $E'$  is the remaining
   edge set, and  $s$  is a start node for breadth-first search
2:  $G' \leftarrow \text{Graph}(V', E')$ 
3:  $G'' \leftarrow \text{Undirected\_Graph}(G')$ 
4:  $E_{max} \leftarrow \emptyset$ 
5:  $T \leftarrow \emptyset$ 
6:  $I \leftarrow \emptyset$ 
7: for each vertex  $u \in V' - \{s\}$  do
8:    $u.color \leftarrow \text{WHITE}$ 
9:    $u.degree \leftarrow 0$ 
10:   $u.receivers \leftarrow \emptyset$ 
11: end for
12:  $s.color \leftarrow \text{GRAY}$ 
13:  $s.degree \leftarrow 0$ 
14:  $Q \leftarrow \emptyset$ 
15:  $\text{Enqueue}(Q, s)$ 
16: while  $Q \neq \emptyset$  do
17:    $u \leftarrow \text{Dequeue}(Q)$ 
18:    $count \leftarrow 0$ 
19:    $I \leftarrow \text{Interference\_Set}(G, T)$ 
20:   for each vertex  $v \in N_{G''}(u)$  do
21:     if ( $v.color = \text{WHITE}$ ) or ( $v.color = \text{GRAY}$ 
       and  $v.degree = 0$ ) then
22:       if  $v \in N_{G'}(u)$  and  $u.degree = 0$  and  $v \notin I$ 
         then
23:          $E_{max} \leftarrow E_{max} \cup \{e_{uv}\}$ 
24:          $v.degree \leftarrow 1$ 
25:          $count \leftarrow count + 1$ 
26:          $u.receivers \leftarrow u.receivers \cup \{v\}$ 
27:       end if
28:        $v.color \leftarrow \text{GRAY}$ 
29:        $\text{Enqueue}(Q, v)$ 
30:     end if
31:   end for
32:   if  $count > 0$  then
33:      $u.degree \leftarrow count$ 
34:      $u.color \leftarrow \text{BLACK}$ 
35:      $T \leftarrow T \cup \{u\}$ 
36:   end if
37: end while
38: return  $E_{max}$ 
39: end function

```

Lines 5-6 make a transmission set and an interference set for a tripartite graph about the relationship between transmitters and interfered vehicles via each transmitter's receivers. In line 5, a transmission set T will contain transmitters in the compatible cover-set in the LoC subgraph G' for the current time slot. In line 6, an interference set I will contain vehicles which get the interference from a transmitter $t \in T$ in the LoC graph G . In lines 7-11, the color and degree of each vertex $u \in V' - \{s\}$ are set to *WHITE* as an unvisited vertex and 0, respectively. Also, the set of u 's receivers (*i.e.*, $u.receivers$)

is set to \emptyset . In lines 12-13, the color and degree of the start node s are set to *GRAY* and 0, respectively. In lines 14-15, a first-in-first-out (FIFO) queue Q is constructed, and the start node s is enqueued for BFS. In lines 16-37, edges $e_{uv} \in E'$ are added to the maximal compatible cover-set E_{max} . In lines 17-18, u is the front vertex dequeued from Q and $count$ for u 's outgoing degree is initialized with 0. Remarkably, in line 19, an interference set I is computed by $\text{Interference_Set}(G, T)$ along with the current transmission set T in the compatible cover-set for a time slot on the LoC graph G . For each transmitter $t \in T$, $\text{Interference_Set}(G, T)$ searches for white, interfered vertices $i \in I$ that are adjacent to t 's receiver in the LoC G . In lines 20-31, for each vertex v that is an adjacent vertex to u in the undirected LoC subgraph G'' , it is determined to add the edge e_{uv} to E_{max} by checking whether or not the receiver v is under the interference of any vertex $i \in I$. In lines 21-30, if v is a white vertex (*i.e.*, unvisited vertex) or a gray vertex with its degree 0 (*i.e.*, visited vertex, but neither transmitter nor receiver), and also if v is an adjacent vertex to u in the directed LoC subgraph G' , u has not yet been selected as a transmitter, and v is not under the interference of any other vertex $i \in I$, then the edge e_{uv} is added to E_{max} , v 's incoming degree is set to 1, u 's outgoing degree increases by 1 with $count$, v is added to the u 's receiver set $u.receivers$, and v is enqueued into Q for the further expansion of the BFS tree. Otherwise, if v is only a white vertex and the condition in line 22 is false, then v is enqueued into Q for the further expansion of the BFS tree. In lines 32-36, if the $count$ is positive, then u 's outgoing degree is set to $count$, and u is added to the transmission set T as a black vertex. Finally, after finishing the while-loop in lines 16-37, a maximal compatible cover-set E_{max} is returned.

REFERENCES

- [1] J. Harding *et al.*, "Vehicle-to-vehicle communications: readiness of V2V technology for application," Nat. Highway Traffic Safety Admin., Washington, DC, USA, Tech. Rep. DOT HS 812 014, 2014.
- [2] Y. L. Morgan, "Notes on DSRC & WAVE standards suite: Its architecture, design, and characteristics," *IEEE Commun. Surveys Tuts.*, vol. 12, no. 4, pp. 504-518, 4th Quart., 2010.
- [3] ASTM International, "Standard specification for telecommunications and information exchange between roadside and vehicle systems - 5 GHz band dedicated short range communications (DSRC) medium access control (MAC) and physical layer (PHY) specifications," ASTM, West Conshohocken, PA, USA, Tech. Rep. ASTM E2213-03(2010), 2010, pp. 1-25.
- [4] *IEEE Standard for Information Technology-Telecommunications and Information Exchange Between Systems Local and Metropolitan Area Networks-Specific Requirements Part 11: Wireless LAN Medium Access Control (MAC) and Physical Layer (PHY) Specifications*, IEEE Standard 802.11-2012 and IEEE Standard 802.11-2007), Mar. 2012, pp. 1295-1303.
- [5] *IEEE Guide for Wireless Access in Vehicular Environments (WAVE)-Architecture*, IEEE Standard 1609.0-2013, Mar. 2014, pp. 1-78.
- [6] S. Eichler, "Performance evaluation of the IEEE 802.11 p WAVE communication standard," in *Proc. IEEE 66th Veh. Technol. Conf.*, Sep. 2007, pp. 2199-2203.
- [7] Z. Wang and M. Hassan, "How much of DSRC is available for non-safety use?" in *Proc. 5th ACM Int. Workshop Veh. Inter-Networking (VANET)*, New York, NY, USA, 2008, pp. 23-29.
- [8] S. Subramanian, M. Werner, S. Liu, J. Jose, R. Lupoiae, and X. Wu, "Congestion control for vehicular safety: Synchronous and asynchronous MAC algorithms," in *Proc. 9th ACM Int. Workshop Veh. Inter-Networking, Syst., Appl. (VANET)*, New York, NY, USA, 2012, pp. 63-72.

- [9] T. V. Nguyen, F. Baccelli, K. Zhu, S. Subramanian, and X. Wu, "A performance analysis of CSMA based broadcast protocol in VANETs," in *Proc. IEEE INFOCOM*, Apr. 2013, pp. 2805–2813.
- [10] K.-T. Feng, "LMA: Location- and mobility-aware medium-access control protocols for vehicular ad hoc networks using directional antennas," *IEEE Trans. Veh. Technol.*, vol. 56, no. 6, pp. 3324–3336, Nov. 2007.
- [11] J.-M. Chung, M. Kim, Y.-S. Park, M. Choi, S. Lee, and H. S. Oh, "Time coordinated V2I communications and handover for WAVE networks," *IEEE J. Sel. Areas Commun.*, vol. 29, no. 3, pp. 545–558, Mar. 2011.
- [12] Y.-B. Ko, V. Shankarkumar, and N. H. Vaidya, "Medium access control protocols using directional antennas in ad hoc networks," in *Proc. IEEE INFOCOM*, vol. 1, Mar. 2000, pp. 13–21.
- [13] Q. Wang, S. Leng, H. Fu, and Y. Zhang, "An IEEE 802.11p-based multichannel MAC scheme with channel coordination for vehicular ad hoc networks," *IEEE Trans. Intell. Transp. Syst.*, vol. 13, no. 2, pp. 449–458, Jun. 2012.
- [14] K. A. Hafeez, L. Zhao, J. W. Mark, X. Shen, and Z. Niu, "Distributed multichannel and mobility-aware cluster-based MAC protocol for vehicular ad hoc networks," *IEEE Trans. Veh. Technol.*, vol. 62, no. 8, pp. 3886–3902, Oct. 2013.
- [15] D. N. M. Dang, C. S. Hong, S. Lee, and E.-N. Huh, "An efficient and reliable MAC in VANETs," *IEEE Commun. Lett.*, vol. 18, no. 4, pp. 616–619, Apr. 2014.
- [16] V. Nguyen, T. Z. Oo, P. Chuan, and C. S. Hong, "An efficient time slot acquisition on the hybrid TDMA/CSMA multichannel MAC in VANETs," *IEEE Commun. Lett.*, vol. 20, no. 5, pp. 970–973, May 2016.
- [17] J. Lee and C. M. Kim, "A roadside unit placement scheme for vehicular telematics networks," in *Proc. LNCS*, vol. 6059, 2010, pp. 196–202.
- [18] P. G. Lopez *et al.*, "Edge-centric computing: Vision and challenges," *SIGCOMM Comput. Commun. Rev.*, vol. 45, no. 5, pp. 37–42, Sep. 2015.
- [19] Garmin Ltd. *Garmin Automotive*, accessed on 2017. [Online]. Available: <https://www.garmin.com/en-US/>
- [20] Waze. *Waze Smartphone App for Navigator*, accessed on 2017. [Online]. Available: <https://www.waze.com>
- [21] T. H. Cormen, C. E. Leiserson, R. L. Rivest, and C. Stein, *Introduction to Algorithms*, 3rd ed. Cambridge, MA, USA: MIT Press, 2009.
- [22] K. Kim, J. Lee, and W. Lee, "A MAC protocol using road traffic estimation for infrastructure-to-vehicle communications on highways," *IEEE Trans. Intell. Transp. Syst.*, vol. 14, no. 3, pp. 1500–1509, Sep. 2013.
- [23] M. S. Sharawi, F. Sultan, and D. N. Aloï, "An 8-element printed V-shaped circular antenna array for power-based vehicular localization," *IEEE Antennas Wireless Propag. Lett.*, vol. 11, pp. 1133–1136, 2012.
- [24] D. Gesbert, M. Kountouris, R. W. Heath, Jr., C.-B. Chae, and T. Sälzer, "Shifting the MIMO paradigm," *IEEE Signal Process. Mag.*, vol. 24, no. 5, pp. 36–46, Sep. 2007.
- [25] N. Razavi-Ghods, M. Abdalla, and S. Salous, "Characterisation of MIMO propagation channels using directional antenna arrays," in *Proc. 5th IEEE Int. Conf. 3G Mobile Commun. Technol.*, Oct. 2004, pp. 163–167.
- [26] V. Kawadia and P. R. Kumar, "Principles and protocols for power control in wireless ad hoc networks," *IEEE J. Sel. Areas Commun.*, vol. 23, no. 1, pp. 76–88, Jan. 2005.
- [27] F. Schmidt-Eisenlohr, M. Torrent-Moreno, T. Mittag, and H. Hartenstein, "Simulation platform for inter-vehicle communications and analysis of periodic information exchange," in *Proc. 4th Annu. Conf. Wireless Demand Netw. Syst. Ser.*, Jan. 2007, pp. 50–58.
- [28] New York State Department of Motor Vehicles. *Driver's Manual*, accessed on 2017. [Online]. Available: <https://dmv.ny.gov/>
- [29] K. Xu, M. Gerla, and S. Bae, "How effective is the IEEE 802.11 RTS/CTS handshake in ad hoc networks," in *Proc. IEEE Global Telecommun. Conf. (GLOBECOM)*, vol. 1, Nov. 2002, pp. 72–76.
- [30] L. G. Roberts, "ALOHA packet system with and without slots and capture," *ACM SIGCOMM Comput. Commun. Rev.*, vol. 5, no. 2, pp. 28–42, 1975.
- [31] W. Crowther, R. Rettberg, D. Waldem, S. Ornstein, and F. Heart, "A system for broadcast communication: Reservation-ALOHA," in *Proc. 6th Hawaii Internat. Conf. Syst. Sci.*, Jan. 1973, pp. 596–603.
- [32] R. K. Lam and P. R. Kumar, "Dynamic channel reservation to enhance channel access by exploiting structure of vehicular networks," in *Proc. IEEE 71st Veh. Technol. Conf. (VTC-Spring)*, May 2010, pp. 1–5.
- [33] *IEEE Standard for Wireless Access in Vehicular Environments (WAVE)—Multi-Channel Operation, 1609 WG—Dedicated Short Range Communication Working Group*, IEEE Standard 1609.4-2016 and IEEE Standard 1609.4-2010, Mar. 2016, pp. 1–94.
- [34] G. Bianchi, "Performance analysis of the IEEE 802.11 distributed coordination function," *IEEE J. Sel. Areas Commun.*, vol. 18, no. 3, pp. 535–547, Mar. 2000.
- [35] J. Hui and M. Devetsikiotis, "A unified model for the performance analysis of IEEE 802.11e EDCA," *IEEE Trans. Commun.*, vol. 53, no. 9, pp. 1498–1510, Sep. 2005.
- [36] Z.-N. Kong, D. H. K. Tsang, B. Bensaou, and D. Gao, "Performance analysis of IEEE 802.11e contention-based channel access," *IEEE J. Sel. Areas Commun.*, vol. 22, no. 10, pp. 2095–2106, Dec. 2004.
- [37] Y. Yao, L. Rao, X. Liu, and X. Zhou, "Delay analysis and study of IEEE 802.11 p based DSRC safety communication in a highway environment," in *Proc. IEEE INFOCOM*, Apr. 2013, pp. 1591–1599.
- [38] OpenStreetMap. *Open Street Map for Road Maps*, accessed on 2017. [Online]. Available: <http://www.openstreetmap.org>
- [39] OMNeT++. *Network Simulation Framework*, accessed on 2017. [Online]. Available: <http://www.omnetpp.org>
- [40] C. Sommer, R. German, and F. Dressler, "Bidirectionally coupled network and road traffic simulation for improved IVC analysis," *IEEE Trans. Mobile Comput.*, vol. 10, no. 1, pp. 3–15, Jan. 2011.
- [41] D. Krajzewicz, J. Erdmann, M. Behrisch, and L. Bieker, "Recent development and applications of SUMO—Simulation of urban MOBility," *Int. J. Adv. Syst. Meas.*, vol. 5, nos. 3–4, pp. 128–138, Dec. 2012.
- [42] T. K. Mak, K. P. Laberteaux, and R. Sengupta, "A multi-channel VANET providing concurrent safety and commercial services," in *Proc. 2nd ACM Int. Workshop Veh. Ad Hoc Netw. (VANET)*, New York, NY, USA, 2005, pp. 1–9.



Jaehoon (Paul) Jeong received the B.S. degree from the Department of Information Engineering, Sungkyunkwan University, in 1999, the M.S. degree from the School of Computer Science and Engineering, Seoul National University, South Korea, in 2001, and the Ph.D. degree from the Department of Computer Science and Engineering, University of Minnesota, in 2009. He is currently an Assistant Professor with the Department of Software, Sungkyunkwan University. His research interests include Internet of Things, vehicular networks, wireless sensor networks, and mobile ad hoc networks. He is a member of the ACM and the IEEE Computer Society.



Yiwen (Chris) Shen received the B.S. degree from the Department of Communication Engineering, North University of China, in 2009, and the M.S. degree from the Department of Mechatronics Engineering, North University of China, in 2013. He is currently pursuing the Ph.D. degree with the Department of Computer Science & Engineering, Sungkyunkwan University, South Korea. His research interests include intelligent transportation systems, vehicular ad hoc networks, and wireless communications. He received the China State Scholarship from the China Scholarship Council.



Sangsoo Jeong received the B.S. degree from the Department of Computer Software, Gachon University, Seongnam, South Korea, in 2013. He is currently pursuing the Ph.D. degree with the Department of Information and Communication Engineering, DGIST. His research areas include cyber-physical systems, smart city, vehicular ad-hoc networks (VANETs), and Internet of Things (IoT).



Sejun Lee received the B.S. degree from the School of Information and Communication Engineering, Mokpo National Maritime University, South Korea, in 2014, and the M.S. degree from the Department of Computer Science and Engineering, Sungkyunkwan University, South Korea, under the supervision of J. Jeong. He is currently a Researcher with the Korea Electronics Technology Institute. His research areas include vehicular ad-hoc networks, cyber-physical systems, and internet of things.

1294
1295
1296
1297
1298
1299
1300
1301
1302
1303
1304
1305



Hwanseok (Harrison) Jeong (S'14) received the B.S. degree from the Department of Computer Engineering, Kyungpook National University, in 1999, and the M.S. degree from the School of Computer Science and Engineering, Seoul National University, in 2001. He is currently pursuing the Ph.D. degree with the Department of Computer Engineering, Sungkyunkwan University. He has been with SK Telecom as a Research and Development Strategist, and the Technical Engineer in Seoul, South Korea, since 2001. His research interests include vehicular ad-hoc networks, mobile ad hoc networks, and cyber-physical systems.

1306
1307
1308
1309
1310
1311
1312
1313
1314
1315
1316
1317
1318



Tae (Tom) Oh (SM'09) received the B.S. degree in electrical engineering from Texas Tech University in 1991, and the M.S. and Ph.D. degrees in electrical engineering from Southern Methodist University in 1995 and 2001, respectively, while working for telecommunication and defense companies. He is currently an Associate Professor with the Department of Information Sciences and Technologies and the Department of Computing Security, Rochester Institute of Technology. His research includes mobile ad hoc networks, vehicle area networks, sensor networks, and mobile device security. He is a member of the ACM.

1319
1320
1321
1322
1323
1324
1325
1326
1327
1328
1329
1330
1331



Taejoon Park (M'05) received the B.S. degree in electrical engineering from Hongik University, Seoul, South Korea, in 1992, the M.S. degree in electrical engineering from the Korea Advanced Institute of Science and Technology Daejeon, South Korea, in 1994, and the Ph.D. degree in electrical engineering and computer science from the University of Michigan, Ann Arbor, MI, USA, in 2005. He is currently a Professor with the Department of Robotics Engineering, Hanyang University, South Korea. His current research interests include in cyber-physical systems, Internet of Things, and their applications to robots and vehicles. He is a member of the ACM.



Muhammad Usman Ilyas received the B.E. degree (Hons.) in electrical engineering from the National University of Sciences and Technology (NUST), Islamabad, Pakistan, in 1999, the M.S. degree in computer engineering from the Lahore University of Management Sciences, Lahore, Pakistan, in 2004, and the M.S. and Ph.D. degrees in electrical engineering from Michigan State University in 2007 and 2009, respectively. He is currently appointed as an Assistant Professor of Electrical Engineering with the School of Electrical Engineering and Computer Science, NUST. He is also an Assistant Professor in the Department of Computer Science in the Faculty of Computing and Information Technology, University of Jeddah in Saudi Arabia.

1332
1333
1334
1335
1336
1337
1338
1339
1340
1341
1342
1343
1344
1345



Sang Hyuk Son (F'13) received the B.S. degree in electronics engineering from Seoul National University, the M.S. degree from KAIST, and the Ph.D. degree in computer science from the University of Maryland at College Park, College Park. He is currently the President of DGIST. He has been a Professor with the Computer Science Department, University of Virginia, and the WCU Chair Professor with Sogang University. His research interests include cyber physical systems, real-time and embedded systems, database and data services, and wireless sensor networks.

1346
1347
1348
1349
1350
1351
1352
1353
1354
1355
1356
1357



David H. C. Du (F'98) received the B.S. degree in mathematics from National Tsing-Hua University, Taiwan, in 1974, and the M.S. and Ph.D. degrees in computer science from the University of Washington, Seattle, in 1980 and 1981, respectively. He is currently the Qwest Chair Professor with the Computer Science and Engineering Department, University of Minnesota, Minneapolis. His research interests include cyber security, sensor networks, multimedia computing, storage systems, and high-speed networking.

1358
1359
1360
1361
1362
1363
1364
1365
1366
1367
1368